

# Graph Neural Networks for Molecules

*A Chapter for Book “Machine Learning in Molecular Sciences”*

Yuyang Wang<sup>12</sup>, Zijie Li<sup>1</sup>, and Amir Barati Farimani<sup>123\*</sup>

1 Department of Mechanical Engineering, Carnegie Mellon University

2 Machine Learning Department, Carnegie Mellon University

3 Department of Chemical Engineering, Carnegie Mellon University

Pittsburgh, PA 15213, USA

{yuyangw,zijieli,barati}@cmu.edu

**Abstract.** Graph neural networks (GNNs), which are capable of learning representations from graphical data, are naturally suitable for modeling molecular systems. This review introduces GNNs and their various applications for small organic molecules. GNNs rely on message-passing operations, a generic yet powerful framework, to update node features iteratively. Many researches design GNN architectures to effectively learn topological information of 2D molecule graphs as well as geometric information of 3D molecular systems. GNNs have been implemented in a wide variety of molecular applications, including molecular property prediction, molecular scoring and docking, molecular optimization and *de novo* generation, molecular dynamics simulation, etc. Besides, the review also summarizes the recent development of self-supervised learning for molecules with GNNs.

---

\* Corresponding author.

## Contents

1	Message Passing Graph Neural Networks . . . . .	1
2	Molecular Graph Neural Networks . . . . .	4
3	Graph Neural Networks on Molecular Applications . . . . .	10
3.1	Molecular Property Prediction . . . . .	10
3.2	Molecular Scoring and Docking . . . . .	13
3.3	Molecular Dynamics Simulation . . . . .	15
3.4	Molecular Optimization and Generation . . . . .	17
	Metrics and Benchmarks . . . . .	17
	Fragment-based Generative Model . . . . .	18
	Molecule-based Generative model . . . . .	20
	Molecular Conformation Generation . . . . .	23
3.5	Others . . . . .	25
	Synthesis Planning and Retrosynthesis Prediction . . . . .	25
	Molecular Knowledge Graph . . . . .	25
	Biomolecules . . . . .	26
4	Self-supervised Learning on Molecule Graphs . . . . .	26
5	Conclusion . . . . .	31

## 1 Message Passing Graph Neural Networks

Graphs are ubiquitous data structure that expresses a set of objects and the relationships between them. Formally, a graph  $\mathcal{G}$  is defined as  $\mathcal{G} = (\mathcal{V}, \mathcal{E})$ , where  $\mathcal{V}$  and  $\mathcal{E}$  denotes the set of objects (nodes) and their relationships (edges), respectively [1]. Fig. 1(a) shows an example of a graph containing four nodes and three edges. Graphs are powerful expressions that can model a wide range of systems. For example, the social network can be modeled as a graph where each node represents a person and each edge represents social connections between them, e.g., friendship, spouseship, colleagueship, etc [2–4]. Other graphical systems include chemical compounds [5, 6], knowledge graphs [7, 8], physical systems [9, 10], and various other domains [11–13]. Recently, there is growing attention from the machine learning (ML) community to develop ML models, especially deep neural networks (DNNs) [14], to analyze graphical data [15, 16]. Previous deep learning models, including convolutional neural networks (CNNs) [17, 18] and recurrent neural networks (RNNs) [19], fail to directly operate on graphical structures. Graph neural networks (GNNs), a deep learning method, are developed to learn representations from graphs directly [20, 21]. GNNs have been prevalent in various domains and many different tasks. In what follows, we will introduce the basic concepts and operations of GNNs.

Modern GNNs are built upon the message-passing layer that aggregates neighboring information to update each node in an iterative manner. The framework is first formalized by Gilmer et al [22]. Let  $\mathcal{G} = (\mathcal{V}, \mathcal{E})$  where the  $i$ -th node is  $u_i \in \mathcal{V}$  and the edge between  $u_i$  and  $u_j$  is  $e_{ij} \in \mathcal{E}$ . Each node  $u_i$  is initialized as a feature vector  $\mathbf{h}_i^{(0)} = \text{Emb}_n(u_i)$  via a node embedding function. Similar to node embedding, each edge  $e_{ij}$  is mapped to a feature vector via an edge embedding function  $\mathbf{a}_{ij} = \text{Emb}_e(e_{ij})$ . The message-passing function is demonstrated in Fig. 1(b). Each message-passing layer contains two operations: (1) computation and aggregation of the messages from neighboring nodes and edges, and (2) update of the node feature based on the message and old feature. The two operations at  $k$ -th layers in a GNN is given in Equation 1 and 2, respectively.

$$\mathbf{m}_i^{(k)} = \sum_{u_j \in \mathcal{N}(u_i)} \phi_m^{(k)}(\mathbf{h}_i^{(k-1)}, \mathbf{h}_j^{(k-1)}, \mathbf{a}_{ij}), \quad (1)$$

$$\mathbf{h}_i^{(k)} = \phi_f^{(k)}(\mathbf{h}_i^{(k-1)}, \mathbf{m}_i^{(k)}), \quad (2)$$

where  $\mathbf{h}_i^{(k)} \in \mathbb{R}^F$  denotes the feature vector of node  $u_i$  at  $k$ -th layer,  $\mathcal{N}(u_i)$  models all the neighbors of node  $u_i$ .  $\phi_m^{(k)}$  and  $\phi_f^{(k)}$  are the message and update functions. By conducting the two operations iteratively, node features within the graph are updated and can be utilized for node-level tasks. To conduct graph-level tasks, like molecular property prediction, directly utilizing all the node features might be infeasible as different graphs have different numbers of nodes. To obtain the representation of the whole graph, the readout operation is introduced to down-sample the node features as illustrated in Fig. 1(c). For a

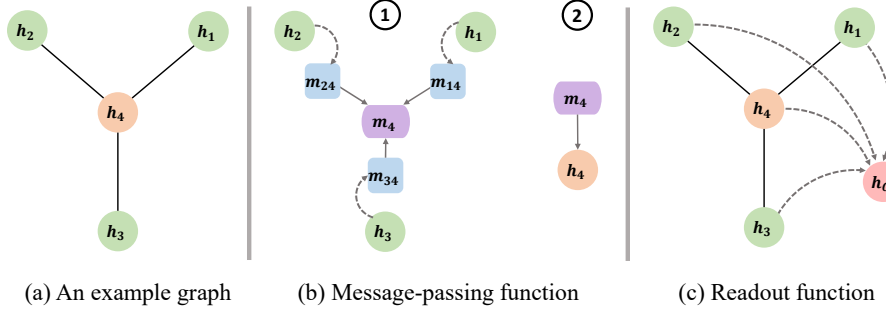


**Fig. 1.** Illustration of (a) an example graph defined by nodes and edges, (b) messaging-passing function containing ① an aggregation operation from  $\mathbf{h}_1$ ,  $\mathbf{h}_2$ , and  $\mathbf{h}_3$  to obtain message  $\mathbf{m}_4$  and ② an update operation to update the node feature  $\mathbf{h}_4$  from  $\mathbf{m}_4$ , and (c) readout function to obtain the graph feature  $\mathbf{h}_G$ .

GNN with  $K$  layers, after the last message-passing layer, the readout function  $R(\cdot)$  is given in Equation 3.

$$\mathbf{h}_G = R(\{\mathbf{h}_i^{(K)} \mid u_i \in \mathcal{V}\}). \quad (3)$$

The design of the message-passing operation is essential to learning graph representations [23]. Since proposed, different GNNs have been developed with different aggregation and update functions for expressive graph representation learning [24–28]. Early spectral methods are built upon the spectral representation of graphs. Such methods compute the eigenvectors of the graph Laplacian for aggregating neighboring information and apply nonlinear activation functions on the aggregated feature to update each node [29, 30]. Graph convolutional network (GCN) [31] introduces a simple yet generic GNN framework, where the aggregation is implemented as an element-wise mean pooling over the node and its neighbors, and the update is implemented as a linear transformation  $\mathbf{W}$  followed by nonlinear ReLU function [32] as given in Equation 4.

$$\mathbf{h}_i^{(k)} = \text{ReLU}(\mathbf{W} \cdot \text{MEAN}(\mathbf{h}_j^{(k-1)} \mid u_j \in \mathcal{N}(u_i) \cup \{u_i\})). \quad (4)$$

GraphSAGE [33] formulates aggregation via multiplication of learnable weight matrix and neighboring features followed by ReLU and max-pooling over the aggregated features as given in Equation 5.

$$\mathbf{h}_i^{(k)} = \sigma \left( \mathbf{W}' \cdot \left[ \text{MAX} \left( \text{ReLU}(\mathbf{W} \cdot \mathbf{h}_j^{(k-1)}) \mid u_j \in \mathcal{N}(u_i) \right) \parallel \mathbf{h}_i^{(k-1)} \right] \right), \quad (5)$$

where  $[\cdot \parallel \cdot]$  is the concatenation and  $\sigma$  is a nonlinear activation function like sigmoid. The update in GraphSAGE contains a concatenation of the node and aggregated features succeeded by a linear transformation  $\mathbf{W}'$ . Equation 6 shows the message-passing in graph isomorphism network (GIN) [34], another widely used GNN architecture. GIN proposes to sum the node features and all the

neighboring features and applies a multi-layer perceptron (MLP) to update the node in the message-passing layer.

$$\mathbf{h}_i^{(k)} = \text{MLP}((1 + \epsilon)\mathbf{h}_i^{(k-1)} + \sum_{u_j \in \mathcal{N}(u_i)} \mathbf{h}_j^{(k-1)}), \quad (6)$$

Further, graph attention network (GAT) [35] introduces the attention mechanism to message-passing via computing the attention score as the weight coefficient in aggregation. The standard attention follows  $\text{Attn}(Q, K, V) = \frac{QK^\top}{\sqrt{d_k}}V$ , where  $Q$ ,  $K$ , and  $V$  are query, key, and value matrices of the embedding of each token, respectively, with the square root of the embedding dimension  $d_k$  as the scaling factor. The message-passing in GAT adjusts the attention as given in Equation 7 and 8.

$$\mathbf{h}_j^{(k)} = \sigma\left(\frac{1}{K} \sum_{k=1}^K \sum_{u_j \in \mathcal{N}(u_i) \cup \{u_i\}} \alpha_{ik}^k \mathbf{W}^k \mathbf{h}_j^{(k-1)}\right), \quad (7)$$

$$\alpha_{ij}^k = \frac{\exp(\text{ReLU}(\mathbf{a}^\top [\mathbf{W}^k \mathbf{h}_i^{(k-1)} \parallel \mathbf{W}^k \mathbf{h}_j^{(k-1)}]))}{\sum_{u_j \in \mathcal{N}(u_i)} \exp(\text{ReLU}(\mathbf{a}^\top [\mathbf{W}^k \mathbf{h}_i^{(k-1)} \parallel \mathbf{W}^k \mathbf{h}_j^{(k-1)}]))}, \quad (8)$$

where  $\alpha_{ij}^k$  is the scalar that measures attention score,  $K$  is the number of attention heads, and  $\mathbf{a} \in \mathbb{R}^{2F}$  is the weight vector. Multiple works also leverage RNNs to model the message-passing function. Gated graph neural networks (GCNN) by Li et al. [25] employs the gated recurrent unit (GRU) [36] to aggregate neighboring information and update node features as shown in Equation 9.

$$\mathbf{h}_i^{(k)} = \text{GRU}\left(\mathbf{h}_i^{(k-1)}, \sum_{u_j \in \mathcal{N}(u_i)} \mathbf{W} \mathbf{h}_j^{(k-1)}\right). \quad (9)$$

Long short-term memory (LSTM) [19] is implemented similarly as GRU for message-passing functions. Tai et al. [37] propose Tree-LSTM that extends LSTM to tree-structured data. Such a model is adapted to general graphs by Peng et al. [38] as well as Zayats and Ostendorf [39].

Recently, there are also efforts on adapting the transformer architecture to graphical data [40]. The standard transformer is designed to learn from sequential data like text [41]. How to encode the structural information of the graph is the major challenge in applying the transformer on graphs. To this end, Graphomer [42] is directly built upon the standard transformer with an effective encoding of the structural information. Specifically, Graphomer includes spatial encoding of the shortest path, edge encoding of edge features on the shortest path, and centrality encoding of the degree centrality of each node. Each encoding is incorporated with learnable parameters and added to the attention score. Dwivedi et al. [43] introduce a graph transformer that learns from the local attention of neighboring connections. It also implements the Laplacian eigenvectors of the graph as the positional encoding in place of sinusoidal positional encoding. Recently, tokenized graph transformer (TokenGT) is proposed to demonstrate that pure transformers can be powerful graph representation learners [44]. Unlike previous works which only tokenize nodes and integrate edge information in attention

updates, TokenGT tokenizes both nodes and edges with orthonormal node identifiers encoding the connectivity of the tokens and trainable type identifiers that encode whether a token is a node or an edge. TokenGT allows adaption of linear attention (e.g., Performer [45]) introduced for pure transformer and reaches  $\mathcal{O}(N+M)$  cost, where  $N$  and  $M$  are the number of nodes and edges, respectively.

For the readout operation, the primitive choices are pooling over all the node features, including mean-pooling, max-pooling, and summation-pooling. Xu et al. [34] point out that summation-pooling is more expressive than mean- and max-pooling, which can capture the full multiset while the other two poolings fail. Works have also investigated other readout functions to improve representation learning and computational efficiency. Attention mechanisms have been implemented in place of summation- or mean-pooling as the readout operation [22, 25]. Vinyals et al. [46] propose set2set function which implements an LSTM for unordered and size-variant input sets. Other methods have probed the rearrangement of the nodes to down-sample the features. Defferrard et al. [30] coarsen the graph into multi-levels via the Graclus algorithm and then rearrange the nodes into a balanced binary tree. The readout is conducted by aggregating the node features in a bottom-up manner. Following the insight, Zhang et al. [47] propose SortPool which ranks nodes based on their structural roles within the input graph and truncates the size of the graph after ranking. DiffPool [48], on the other hand, develops a differentiable pooling module that generates hierarchical graph representations. It learns a soft clustering assignment at each layer to aggregate node features. SAGPool [49] combines self-attention with end-to-end hierarchical representation learning which includes both node feature and graph topology. In general, the readout operation can be considered as a special message-passing layer that aggregates all the updated node features within the graph. It also plays an important role in learning expressive graph representations.

## 2 Molecular Graph Neural Networks

The previous section has introduced the basic concepts of the message-passing GNN and its prevalent variants. This section focuses on the GNN architectures that are adapted and designed for molecular representation learning. As the focus of this chapter, molecules, can be naturally viewed as graphs [50]. Fig. 2 illustrates examples of how molecule graphs are built. Within the graph, each node models an atom, and each edge models the interatomic interactions. Interactions include two-dimensional (2D) topological information like covalent bonds and 3D geometric information like distances and angles. Graph representations have demonstrated advantages over other molecular featurization techniques. Some methods develop a language that converts a molecule into a one-dimensional (1D) string, e.g., simplified molecular-input line-entry system (SMILES) [51], SMILES arbitrary target specification (SMARTS) [52], and recently developed self-referencing embedded strings (SELFIES) [53]. Other works propose rules that can embed each molecule into a feature vector, namely a molecular finger-

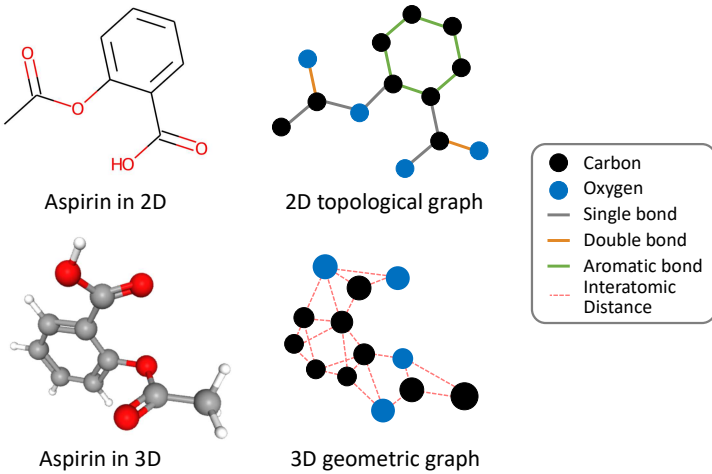


**Fig. 2.** Illustration of building graphs from molecules using 2D topological and 3D geometric information. The aspirin molecule is shown as an example.

print or a descriptor, that usually encodes the presence or absence of certain substructures in the molecule. Examples include extended-connectivity fingerprint (ECFP) [54] and molecular access system (MACCS) keys [55]. Both string-based and fingerprint-based methods have been widely and successfully implemented in many applications including molecular similarity search, clustering, and virtual screening. With the rise of deep learning in recent years, deep learning methods have been applied to learn molecular representations from molecular languages and fingerprints. Though these featurization techniques follow certain rules to encode substructure information, they, however, still struggle to directly model the topological and geometric information of molecules. GNNs, which learn representation from molecule graphs, are capable of encoding the graphical structures. Many works have investigated the GNN architectures for learning from molecule graphs. Also, atomic and bond descriptors, like atomic number, charge, chirality, hybridization, bond type, etc., can be added to the node and edge features. This chapter focuses on the message-passing architecture design for molecule graphs.

Duvenaud et al. [5] introduce one of the pioneering works that learning molecular representations via a GNN. In this work, node features are aggregated through concatenation and are updated through a learnable matrix conditioned on the node degree followed by a sigmoid function. The readout operation computes a weighted summation over node features from all the layers. Another trailblazing model, named Weave, from Kearnes et al. [6] proposes molecular graph convolutions that update edge features in each message-passing layer. Specifically, at each layer, one first updates the edge features from connected nodes and then updates the node features by aggregating the edges. Hu et al.

[56] extend the standard GIN by including the edge features in message-passing as given in Equation 10.

$$h_v^{(k)} = \text{MLP} \left( h_v^{l-1} + \sum_{u_j \in \mathcal{N}(u_i)} (h_j^{(k-1)} + a_{ij}) \right), \quad (10)$$

where  $a_{ij}$  is the embedding of the edge between nodes  $u_i$  and  $u_j$ , containing the information of bond type and direction. Glimer et al. [22] elucidate a simple yet unified GNN framework named message passing neural network (MPNN) which most of the previous models fall into. They then propose enn-s2s, a variant of MPNN that aggregates neighboring information as given in Equation 11.

$$a_i^{(k)} = \sum_{u_j \in \mathcal{N}(u_i)} \text{MLP}(a_{ij}) h_j. \quad (11)$$

Besides, it follows set2set [46] as the readout function to obtain molecule representations. Yang et al. [57] further proposed directed MPNN (D-MPNN) that uses information associated with directed edges instead of information associated with vertices in standard MPNN. In addition, D-MPNN implements rich atom and bond features to improve the expressiveness of molecule graphs. Attention mechanisms have been developed for molecular GNNs. Xiong et al. [58] introduce AttentiveFP containing atom embedding layers and molecule embedding layers. The atom embedding layers borrow the attention mechanism introduced in GAT to aggregate local messages and the output attention context is fed into a gated recurrent unit (GRU) together with atom features from the previous layer to obtain updated context. The molecule embedding layers assume a virtual node that connects to all atoms and follows the same pattern as atom embedding layers. The final output of the virtual node is used as the representation of the whole molecule graph. Not only the attention mechanisms but also the transformer architectures are investigated for molecule graphs. Rong et al. [59] introduce GTransformer which combines the message-passing framework with transformer. GTransformer applies a bi-level message-passing strategy that aggregates and updates the information on both nodes and edges. Besides, it employs the residue connection and dynamic message-passing by randomly choosing the number of aggregation hops.

So far, we have discussed GNNs that model molecules as 2D graphs. Namely, these models only consider topological information while ignoring geometric information like distances and angles in the 3D Euclidean space. Such 2D GNNs have demonstrated promising performance in many applications. However, 3D information is crucial as it is closely related to the energy landscape and molecules rely on 3D conformation to function in practice. Nevertheless, simply adding the positional coordinates into GNNs can be problematic as translation or rotation of the molecule will change the output of the models. One would expect to design GNN architectures whose output is immutable to the rotations and translations of 3D molecular structures [60]. To formalize, we borrow the concept from group theory and denote the set of proper rigid transformations (i.e., translations and rotations) in  $n$ -dimensional Euclidean space as  $\text{SE}(n)$  [61]. Many works thus

explore SE(3)-invariant GNNs for molecules existing in 3D Euclidean space. Schütt et al. [62] introduce the deep tensor neural network (DTNN) that model the distances between atoms in message-passing. DTNN extract the graph-level representation by feeding each node feature into an MLP and summing them up. Following DTNN, Schütt et al. further propose SchNet [63] that is composed of well-designed layers to model local correlations between atoms. Equation 12 elaborate the atom-wise update while Equation 13 and 14 elaborate continuous-filter convolution at the  $(l+1)$ -th layer in SchNet.

$$h_i^{(k)} = Wh_i^{(k)} + b \quad (12)$$

$$h_i^{(k)} = \sum_{u_j \in \mathcal{N}(u_i)} h_j^{(k)} \circ W_{\text{cf}}^{(k-1)}, \quad (13)$$

$$W_{\text{cf}}^{(k)} = \text{SoftPlus}(W_2^{(k)} \cdot \text{SoftPlus}(W_1^{(k)} \cdot \parallel_{u_j \in \mathcal{N}(u_i)} \text{RBF}(d_{ij}))), \quad (14)$$

where  $\circ$  is an element-wise multiplication,  $d_{ij}$  is the distance in Euclidean space between nodes  $u_i$  and  $u_j$ , and  $\text{RBF}(d_{ij}) = \parallel_{k=1}^K \exp(-\gamma \|d_{ij} - \mu_k\|^2)$  concatenates radial basis functions with  $\mu_k = 0.1k\text{\AA}$  and  $\gamma = 10\text{\AA}$  that expands the interatomic distance from a scalar to a vector of  $\mathbb{R}^K$ . Besides, it implements SoftPlus, a smooth approximation to ReLU, as nonlinear activation functions. Each message-passing layer starts with an atomise-wise update followed by a continuous-filter convolution operation. It then conducted two atom-wise updates with a SoftPlus activation in between to obtain the combination term  $v_i^{(k)}$ . The final output node feature at the  $(l+1)$ -th layer is updated by  $h_i^{(k+1)} = h_i^{(k)} + v_i^{(k)}$ . SchNet effectively encodes 3D distance information to molecular GNN and inspires many follow-up works in this domain. PhysNet by Unke et al. [64] also leverages the interatomic distances to build an SE(3)-invariant GNN, which adapts the interaction blocks to update node features from distances and the residual blocks to learn representations with deeper neural networks. DimeNet by Gasteiger et al. [65] follows the architecture of PhysNet while integrating additional angular information expanded with Fourier-Bessel representations. The message-passing at the  $k$ -th layer from node  $u_j$  to  $u_i$  takes in not only the distance  $d_{ij}$  but also angles  $\angle_{u_k u_j u_i}$  as well as  $h_k^{(k-1)}$ , where  $u_k \in \mathcal{N}(u_j) \setminus \{u_i\}$ . The same team further proposes an improved version named DimeNet++ [66] with fast interactions and embedding hierarchy. Fang et al. [67] report GeoGNN containing the atom-bond graph and bond-angle graph to incorporate both interatomic distances and angles. In the atom-bond graph, each node represents an atom and each edge represents a covalent bond, while in the bond-angle graph, each node represents an atom-pair and each edge represents the angle between two pairs. GeoGNN builds the message-passing function based on GIN [34] and updates the atom-bond and bond-angle graphs iteratively. Adams et al. [68] introduce a model that is invariant to rotations of rotatable bonds.

Though SE(3)-invariant has merits for GNN in various molecular property predictions, it is still limited for expressing graph representations in some aspects. One limitation is that such invariance requires the message-passing to

contain only features of distances or angles but is unable to encode directional information. Besides, for applications like force field prediction where the output is expected as a set of 3D vectors, SE(3)-invariant GNNs give the same output for molecules with different rotations in 3D. However, the force field is expected to rotate together with the rotation of the molecular system. To this end, SE(3)-equivariance is introduced which generalizes the concept of invariance. Formally, equivariance is a kind of symmetry for function. For function  $\Phi : \mathcal{X} \rightarrow \mathcal{Y}$  (e.g.,  $\Phi$  can be a deep neural network), it is equivariant with respect to group  $G$  such that it commutes with any group actions  $g \in G$  on  $\mathcal{X}$  and  $\mathcal{Y}$  as shown in Equation 15.

$$\rho_g^{\mathcal{Y}}(\Phi(x)) = \Phi(\rho_g^{\mathcal{X}}(x)), \forall x \in \mathcal{X}, g \in G, \quad (15)$$

where  $\rho^{\mathcal{X}}(g)$  and  $\rho^{\mathcal{Y}}(g)$  are the group representation of group action  $g$  on  $\mathcal{X}$  and  $\mathcal{Y}$  space, respectively. The group representation of group action  $g \in G$  on vector space  $\mathcal{V}$  is defined as:

$$\rho : G \mapsto GL(V), \quad (16)$$

such that  $\rho(g_1g_2) = \rho(g_1)\rho(g_2), \forall g_1, g_2 \in G$  (function satisfies this property is called group homomorphism). The group representation allows operating abstract mathematical object-group action, on the vector space of particular interest. More specifically, for 3D molecules' modeling, we are interested in studying the equivariance with respect to 3D rotations/translations, which corresponds to the 3D special Euclidean group, SE(3). A useful property of the equivariant functions is that composing them will yield another equivariant function, which means the whole network is equivariant if each layer is equivariant. In addition, translation invariance (invariance is also equivariance) is straightforward to achieve in most neural networks as long as they do not use global coordinates as features. Therefore in most of the models, the 3D rotation group SO(3) is the only group that requires special care.

The first major category of equivariant networks is based on irreducible representation, tensor product, and spherical harmonics. For 3D rotations, its representations are orthogonal matrices and can always be decomposed into the irreducible representation of the following form:

$$\rho(g) = Q^T \left[ \bigoplus_l D^{(l)}(g) \right] Q, \quad (17)$$

where  $Q$  is an  $N \times N$  orthogonal matrix (for change of basis),  $\bigoplus$  is the direct sum, and  $D^{(l)}(g)$  is the *Wigner D-matrices* for group action  $g$  [69]. Vectors transformed under  $D^{(l)}(g)$  are called  $l$ -th order vectors, which have a length of  $2l + 1$ . Based on these representations, useful learnable equivariant layers can be developed. A common recipe is first building learnable filters with spherical harmonics and then composing them with input features through the tensor product, which ascribes to the fact that spherical harmonics are the equivariant basis for SO(3) and the tensor product is equivariant. Moreover, the tensor product of the irreducible representations of the vector space can be evaluated by

looking up a set of pre-calculated coefficients, which are called Clebsch-Gordon coefficients.

Tensor Field Network [10] proposes a  $\text{SO}(3)$  equivariant layer under this recipe:

$$h_{\text{out},i}^l = W^{ll} h_{\text{in},i}^l + \sum_{k \geq 0} \sum_{j \in \mathcal{N}(i)}^n W^{lk}(\vec{r}_j - \vec{r}_i) h_{\text{in},j}^k, \quad (18)$$

where  $h_i^l$  denotes the  $l$ -th order vector of input/output features,  $W^{lk}(\vec{r}_j - \vec{r}_i)$  is a learnable filter conditioned on relative position  $\vec{r}_j - \vec{r}_i$ . More specifically, the learnable filter is derived by multiplying a learnable scalar with Clebsch Gordon coefficients and spherical harmonic basis function:

$$W^{lk}(\vec{r}_j - \vec{r}_i) = \sum_{J=|k-l|}^{k+l} \psi_J^{lk}(\|r_{ij}\|) \sum_{m=-J}^J Y_m^{(J)} \left( \frac{\vec{r}_j - \vec{r}_i}{\|r_{ij}\|} \right) Q_{Jm}^{lk}, \quad (19)$$

where  $\psi_J^{lk}(\cdot)$  is a learnable function conditioned on the interatomic distance:  $\|r_{ij}\| = \|\vec{r}_j - \vec{r}_i\|_2$ ,  $Y_m^{(J)}$  denotes the  $m$ -th dimension of  $J$ -th spherical harmonics, and  $Q_{Jm}^{lk}$  denotes the  $(J, m)$ -th coefficient in Clebsch-Gordon matrice. The composed learnable filter  $W^{lk}(\vec{r}_j - \vec{r}_i)$  with a shape  $(2l+1) \times (2k+1)$  will map type- $k$  features to type- $l$  features. Tensor Field Network, there is an active line of works [70–72] in using operation on irreducible representation to build  $\text{SE}(3)$  equivariant network.

Another direction to build an equivariant network is to exploit the properties of vectorial features instead of leveraging tools from group representation theory. The principle is that the operation on the directional features (e.g. velocities) can only be linear. Therefore, when building the message passing layer, the operations on vector features  $\vec{h}$  are restricted to: (a) Linear projection  $W\vec{h}$ ; (b) Dot product:  $\langle \vec{h}_1, \vec{h}_2 \rangle$ ; (c) Tensor product:  $\vec{h}_1 \otimes \vec{h}_2$ . An example of a such recipe is PaiNN [73], where it proposes an equivariant message passing block by extending the continuous and invariant message passing layer proposed in [63]. Each layer in the PaiNN comprises two sub-blocks, a message passing block, and an update block. Inside the message passing block, the update of scalar features  $\Delta s_i$  are calculated as:

$$\Delta s_i = \sum_{j \in \mathcal{N}(i)} \phi_s(s_j) \odot W_s(\|r_{ij}\|), \quad (20)$$

where  $\odot$  denotes Hadamard product,  $\phi_s(\cdot)$  is a learnable atom-wise function,  $W_s(\|r_{ij}\|)$  is the learnable continuous filter conditioned on interatomic distance, which is a linear combination of the radial basis function (PaiNN adopts the radial basis function proposed in [74]). Similarly, the update of vector features

is defined as:

$$\Delta \vec{h}_i = \sum_{j \in \mathcal{N}(i)} \vec{h}_i \odot \phi_{vv}(s_j) \odot W_{vv}(\|r_{ij}\|) \quad (21)$$

$$+ \sum_{j \in \mathcal{N}(i)} \phi_{vs}(s_j) W_{vs}(\|r_{ij}\|) \frac{\vec{r}_j - \vec{r}_i}{\|r_{ij}\|}, \quad (22)$$

where the first half of the equation is a convolution with respect to the vector features, and the second half is a convolution with respect to the scalar features using an equivariant filter. After the message passing block, the scalar and vector features are updated with the calculated residuals:  $s_i \leftarrow s_i + \Delta s_i$ ,  $\vec{h}_i \leftarrow \vec{h}_i + \Delta \vec{h}_i$  and then fed into update block. Next, in the update block, the update of scalar features is calculated as:

$$\Delta s_i = a_{ss}(s_i, \|W_v \vec{h}_i\|) + a_{sv}(s_i, \|W_v \vec{h}_i\|) \langle W_u \vec{h}_i, W_v \vec{h}_i \rangle, \quad (23)$$

where  $a_{ss}$  and  $a_{sv}$  are learnable function, and  $W_v, W_u$  are learnable linear projection matrices. And then the update of vector features is calculated as:

$$\Delta \vec{h}_i = a_{vv}(s_i, \|W_v \vec{h}_i\|) W_u \vec{h}_i. \quad (24)$$

In practice,  $a_{ss}, a_{sv}, a_{vv}$  are derived from the same network  $a$  by splitting along the feature dimension of output. The scalar features and vector features are again updated with residuals. Equivariant Transformer [75] extends the above message passing layer to attention. GVP-GNN [76] leverages a similar idea with different design choices of the message passing layer. As demonstrated in Soledad Villar et al. [77], such formulation is expressive enough for approximating SE(3) equivariant functions.

It is worth noting that the above models are just non-exhaustive instances of equivariant graph neural networks. There are several other lines of works that leverage different principles such as Lie algebra [78, 79], or other message passing protocols designed for vector features [80–83] and more general groups [84].

### 3 Graph Neural Networks on Molecular Applications

GNNs have been widely implemented to various applications in molecular sciences [85–87]. This section reviews the molecular applications empowered by GNNs, including molecular property prediction, molecular scoring and docking, molecular dynamics simulation, molecular optimization and generation, and others. Each subsection introduces the formulation of the problem, prevalent datasets and metrics, as well as works to solve the problem using GNNs.

#### 3.1 Molecular Property Prediction

The most straightforward utilization of GNNs is to predict the molecular properties given the molecule graphs [86]. Such a task can be considered as a graph

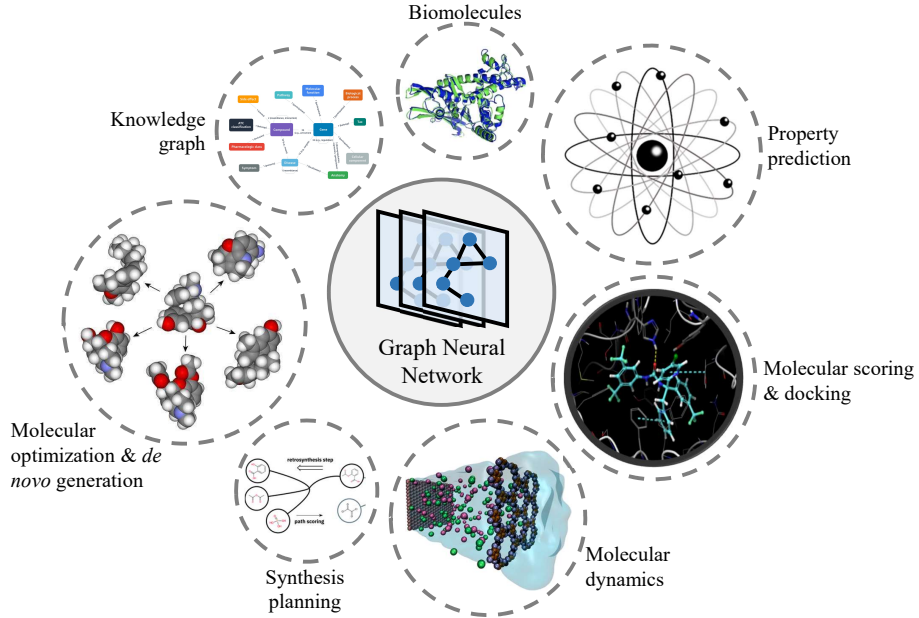


**Fig. 3.** Various applications of GNNs on molecular sciences.<sup>1</sup>

classification or regression following the empirical risk minimization in supervised learning. For a dataset of  $N$  molecule graph and property pairs  $\{(\mathcal{G}_1, y_1), \dots, (\mathcal{G}_N, y_N)\}$ , the objective to optimize is given in Equation 25.

$$\min_{\theta} \sum_i \ell(\text{GNN}_{\theta}(\mathcal{G}_i), y_i), \quad (25)$$

where  $\text{GNN}_{\theta}(\cdot)$  is a GNN model parameterized by  $\theta$  to predict a certain property from an input molecule graph  $\mathcal{G}_i$  and  $\ell(\cdot, \cdot)$  measures the difference between the prediction and ground truth label, like cross-entropy loss for classification tasks and mean squared error for regression tasks [88–90]. Researchers have collected multiple databases containing a wide variety of molecular properties so that different GNN models can be benchmarked. Table 1 summarizes the domain, the number of compounds, the number of tasks, task type, whether containing 3D information and the sources of the popular databases for molecular property predictions. MoleculeNet [93] is a widely used benchmark for molecular property prediction built upon multiple public databases. It contains multi-level properties, including physiology, biophysics, physical chemistry, and quantum mechanics. Besides, benchmarking-GNN [94] creates ZINC

<sup>1</sup> Resources of some fragments in Fig. 3: [91–93], <https://www.dgl.ai/news/2020/06/09/covid.html>, [https://www.gla.ac.uk/news/archiveofnews/2021/september/headline\\_812517\\_en.html](https://www.gla.ac.uk/news/archiveofnews/2021/september/headline_812517_en.html), <https://www.deepmind.com/blog/alphafold-a-solution-to-a-50-year-old-grand-challenge-in-biology>.

and AQSOL datasets for predicting the constrained and aqueous solubility. It should be pointed out that benchmarking-GNN only uses a subset of the original ZINC database (250,000 molecules) [95]. Recent efforts have focused on generating labeled molecular datasets via density functional theory (DFT) calculations. QM9, which is also included in MoleculeNet, contains approximately 134k molecules with their geometric, energetic, electronic, and thermodynamic properties. Alchemy [96] extends the previous dataset to include 12 quantum mechanical properties of 119,487 molecules with up to 14 heavy atoms. PCQM4M and its latest version PCQM4Mv2 in the OGB challenge aim at predicting the DFT-calculated HOMO-LUMO energy gap from 2D or 3D molecule graphs. ANI-1 [97] extends this concept of such datasets by including the energies of off-equilibrium conformations. Specifically, ANI-1 contains 24,687,809 conformations from 57,462 molecules. There are also works that create curated datasets for specific tasks, including quantitative structure-odor relationship (QSOR) [98], Carbon absorption [99], etc. Molecular property prediction is challenging since different datasets in it have numbers of instances of different magnitudes, from less than 200 to about 4,000,000 molecules. Also, most classification tasks in it have quite imbalanced labels, therefore, ROC-AUC and PRC-AUC are widely used instead of accuracy to measure the performance of different models. Regression benchmarks adapt either root-mean-square error (RMSE) or mean absolute error (MAE) as evaluation metrics. Besides, Hu et al. [93] introduce scaffold splitting to separate structurally different molecules into training, validation, and test subsets. This strategy provides a more challenging yet realistic setting than random splitting and has been leveraged in many works on molecular property prediction [56–59, 67, 100].

Most of the GNN architectures introduced in Section 1 and 2 can be leveraged on molecular property predictions. Apart from those models, a wide range of GNN variants have been developed for the application. Wieder et al. [86] provide a comprehensive survey for the molecular property predictions via GNNs till the year 2020. Early works utilize spectral GNNs for molecular property prediction [124–127]. Since the proposal of GCN [31], a simple yet generic algorithm, many GNNs have been built upon it for molecular property predictions [128–132]. Some works have also explored using RNNs for aggregation in this area [133–135]. After the formalization of the message-passing framework by Gilmer et al. [22], researchers have built GNNs systematically following the insight to predict a wide range of molecular properties [57, 136–138].

Recently, there are emerging researches that leverage DNNs, especially SE(3)-invariant or SE(3)-equivariant GNNs with 3D geometric information, for quantum mechanics (QM) predictions [139–141]. Many works are evaluated on QM9. Early SE(3)-invariant GNNs, including SchNet [63], PhysNet [64], HIP-NN [142], MGNC [143], DimeNet [65], DimeNet++ [66], Cormorant [144], SphereNet [145], are built upon interatomic distances and angles. Some works have leveraged orbital information to better predict QM properties [146–149]. GNNs built upon SE(3)-equivariant operations have also been widely applied to this application. Examples include SE(3)-Transformer [70], E(n)-GNN [150], LieTransformer

Domain	Dataset	# Molecules	# Tasks	Task type	3D	Source
Physiology	MUTAG	188	1	Classification	No	[101]
	SIDER	1,427	27	Classification	No	[93, 102]
	ClinTox	1,478	2	Classification	No	[93, 103]
	BBBP	2,039	1	Classification	No	[93, 104]
	NCI1	4,110	1	Classification	No	[105]
	Tox21	7,831	12	Classification	No	[93, 106]
	ToxCast	8,575	617	Classification	No	[93, 107]
Biophysics	BACE	1,513	1	Classification	No	[93, 108]
	CCRF-CEM	3,047	1	Regression	No	[109]
	PC-3	4,294	1	Regression	No	[109]
	PDBBind	19,443	1	Regression	Yes	[93, 110, 111]
	HIV	41,127	1	Classification	No	[93, 112]
	MUV	93,087	17	Classification	No	[93, 113]
Physical Chemistry	PCBA	437,929	128	Classification	No	[93, 114]
	FreeSolv	642	1	Regression	No	[93, 115]
	ESOL	1,128	1	Regression	No	[93, 116]
	Lipophilicity	4,200	1	Regression	No	[93, 117]
	AQSOL	9,982	1	Regression	No	[94, 118]
Quantum Mechanics	ZINC	12,000	1	Regression	No	[94, 95]
	QM7	7,165	1	Regression	Yes	[93, 119]
	QM7b	7,211	14	Regression	Yes	[93, 120]
	QM8	21,786	12	Regression	Yes	[93, 121]
	QM9	133,885	12	Regression	Yes	[93, 122]
	Alchemy	119,487	12	Regression	Yes	[96]
	PCQM4M	3,803,453	1	Regression	No	[123]
	PCQM4Mv2	3,378,606	1	Regression	Yes	[123]
ANI-1		24,687,809 (conf.)	1	Regression	Yes	[97]

**Table 1.** Summary of benchmarks for molecular property predictions.

[151], L0/L1Net [152], GemNet [153], PaiNN [154], and TorchMD-Net [75]. Many SE(3)-equivariant GNNs have also been benchmarked MD17 [155] which contains energy and force field predictions from molecular dynamics simulations of eight molecules. We will discuss GNN applications on MD simulations in Section 3.3 extensively. Recent works have investigated *ab-initio* solution of the Schrödinger equation to acquire fundamental QM properties equipped with GNNs. Hermann et al. [156] propose PauliNet, a GNN-based wave function ansatz. PauliNet adapts SchNet as the GNN backbone and exploits multireference Hartree-Fock solution as the optimization start point. The whole framework is trained using variational quantum Monte Carlo (VMC). Gao et al. [157] introduce a framework combining a GNN and a neural wave function to solve the Schrödinger equation for multiple geometries via the VMC method simultaneously.

### 3.2 Molecular Scoring and Docking

Molecular scoring mainly refers to the prediction of pharmacological activity of a molecule candidate, which is essential in *in silico* drug discovery [87]. Such a method is widely applied in the virtual screening of drug candidates. It can also

be leveraged to narrow down the search space for *de novo* molecular generation. There are two major categories of molecular scoring: ligand-based scoring and structure-based scoring. The ligand-based scoring requires no information about the receptor in pharmacological activities. Such a setting can be considered as a special case of molecular property predictions that model the quantitative structure-activity relationships (QSAR), like drug-likeness, toxicity, solubility, etc. On the contrary, structure-based scoring is based on the structure of the biological target (usually a protein) of a molecule. Such a strategy predicts the drug-target interactions given the drug candidates and the target receptors. Molecular docking predicts the preferred pose of a molecule when bound with a binding site to form a stable protein-ligand complex. It is one of the most popular techniques in structure-based drug discovery. Several works leverage 3D CNN to model the protein-ligand complex [158–162]. However, 3D CNN requires voxelization of 3D space which adds burdens to the memory. Moreover, such a voxelization loses resolution of the exact pose in 3D and lacks explicit modeling of interatomic interactions. This chapter reviews the structure-based molecular scoring and molecular docking empowered by GNNs.

PDBBind [110, 163, 164] collects biomolecular complexes with their experimental binding affinity data and is widely used in structure-based scoring with deep learning as a regression task. DUD-E [165] is another dataset that contains 102 targets across different protein families. For each target, both positive (active) and negative (decoy) ligands are provided, which are formalized as classification tasks. Also, BindingDB [166, 167] is a public database of measured binding affinities of proteins and ligands. Drugbank [168, 169], a public online database, that collects FDA-approved drugs with drug target and drug action information. ChEMBL [117] also provides plenty of protein-ligand information including chemical compound and activity assay data. Several works have also created curated databases [170, 171].

Structure-based scoring aims at predicting the binding affinity of drug-target interactions (DTIs) [172]. The key to designing GNN models for structure-based molecular scoring is how to integrate the information of the protein and/or the binding pocket to the ligand [173–175]. Feinberg et al. [176] introduce PotentialNet, a pioneering GNN framework that models the protein-ligand complexes. PotentialNet takes two stages in message-passing: (1) intra-molecular message-passing based only on covalent bonds, and (2) intra- and inter-molecular message-passing based on Euclidean distance and bonds. Gomes et al. [177] introduce a framework contain three parameter-sharing Siamese GNNs that encode ligand, protein, and protein-ligand complex, to features  $G_{\text{ligand}}$ ,  $G_{\text{protein}}$ , and  $G_{\text{complex}}$ , respectively. The prediction of binding affinity then utilizes  $\Delta G = G_{\text{complex}} - G_{\text{ligand}} - G_{\text{protein}}$ . Lim et al. [178] improve the framework by conducting intra-molecular message passing and inter-molecular massage-passing simultaneously. The model utilizes the subtraction between the features of a target protein and the ligand in their complex to predict the binding affinity. Such a strategy that models the interactions within the ligands and interactions between ligands and targets is widely used in later works. InteractionGraphNet

[179] by Jiang et al. models the intra- and inter-molecular interactions sequentially with two independent GNN models. Morrone et al. [180] adapt a dual-GNN framework to encode the ligand graph and protein-ligand interactions separately. The output of the two GNNs is concatenated and fed to an MLP to predict the binding affinity of the complex. Son et al. [181] propose GraphBAR, a framework containing multiple graphs whose adjacency matrices cover neighbors within different distance cutoffs. Knutson et al. [182] propose two parallel GNNs with one incorporating domain knowledge of proteins and ligands while the other learning interactions with no domain prior. The works listed above are built upon protein-ligand complexes. However, these models may suffer to make accurate predictions for those complexes without experimental measurements. To this end, Torng and Altman [183] propose to encode protein pocket graphs and 2D molecule graphs independently and combine the output features to predict the DTIs. Recent works have introduced language models to encode protein information in predicting DTIs [170, 184–188].

Unlike structure-based scoring which predicts binding affinity directly, molecular docking focuses on predicting the posture of a protein-ligand complex. Conventional docking contains a search module to generate massive potential protein-ligand binding poses and a scoring module to evaluate the interaction of binding poses [189–191]. Such methods rely on heavy candidate sampling and usually involve empirical scoring functions, thus may be time-consuming and inaccurate [192, 193]. Recently, there are emerging works that apply GNNs for molecular docking [194–197]. Jiang et al. [198] develop a GNN to refine the initial docking pose from conventional docking software. The GNN can be run multiple times to gradually get optimal predictions. Mendez et al. [199] report DeepDock, which first learns a statistical potential based on distance likelihood and then samples ligand conformations based on learned potential. Specifically, DeepDock models statistical potentials on torsion angles to generate favorable molecular conformations in the binding site [200]. However, these methods assume prior knowledge of the binding site for the ligands. Some works have investigated predicting protein binding sites using GNNs [11, 201–204]. To this end, GNN methods have been developed to both locate the binding site and predict the preferred binding conformations. EquiBind [205] by Stärk et al. adapts SE(3) GNN to predict the binding site and applies constraints that only allow change of torsion angles while keeping bond lengths and angles fixed. TANKBind [206] by Lu et al. incorporates trigonometry constraints to GNNs which avoid unrealistic conformations like atom overlapping. It also leverages contrastive learning to build the energy landscape for the inter-molecular interaction of different binding sites.

### 3.3 Molecular Dynamics Simulation

Molecular Dynamics (MD) has a wide range of applications in material science, chemistry, and biophysics [207–209]. It provides a numerical way to study and predict intricate molecular systems. In essence, MD simulation calculates atomic forces and then updates the system states with a discretized equation of motion.

The forces can either be modeled by ab initio approaches (AIMD) like density functional theory (DFT) [210] that considers the electronic structure of atoms or through empirical potentials (classical MD) which bypasses electronic structures [211]. AIMD is highly accurate but its computation is prohibitively expensive, which limits its scope of application. On the contrary, classical MDs are much more efficient, yet with worse accuracy and limited generalizability. The major limitation of classical MD simulations stems from the difficulty in how to describe complex interatomic potentials accurately with the appropriate functional form given the diverse types of interactions in the system. In this regard, neural networks have the potential to close the accuracy gap between classical MD and AIMD with its function approximation capability [212–216].

Depending on how the environment of the atom is described, neural networks can be categorized into two broad categories. The first kind of approach relies on hand-designed featurization, which builds tailored descriptors that exploit domain knowledge [139, 212, 217–220]. One of the first examples is Behler-Parrinello Neural Networks (BPNN) [221–223], which proposes atom-centered symmetry functions (ACSFs) for describing the local neighborhood around an atom. Graph neural networks, on the other hand, provide a framework to directly learn the atomic representations from the raw atomic coordinates and low-level atomic features, offering an alternative to the manually tailored atomic descriptors [5, 22, 62–64, 73, 74].

Based on the above frameworks, neural networks can be used to address the efficiency-accuracy tradeoff in MD from the following aspects. The first aspect is to use neural networks to learn the forcefield (i.e. interatomic potential) of a molecular system. In this case, neural networks trained on data with ab initio level accuracy can serve as fast and efficient surrogate models for AIMD. The output of the network can either be the potential energy surface (PES) or atomic forces, in turn forming an energy-based model (also known as neural network potentials) [62, 63, 74, 139, 155, 223–227] or force-based model [228–231]. These two variants are similar in principle (Chmiela et al. [155] demonstrate that force-based model essentially learns a linearization of the PES), but force-based models are more accurate at predicting forces in practice and can bypass the process of calculating energy gradients. However, force-based models are generally not energy conserving and thus can generate unphysical predictions. Another perspective is learning the pattern of molecular trajectories instead of the dynamics, which treats the simulation as a sampling problem. Here neural networks are used as a probabilistic generative model [232–235] to model the distribution  $p(x_{t+1}|x_t)$  with  $x_t$  denotes the state of the system at time  $t$ . Since this paradigm no longer depends on dynamics to update the system, it does not suffer from the truncation error that arises from the discretization error of the equation of motion and thus can adopt a very large time step size (e.g. at the scale of a nanosecond). The downside is such a method can lead to unphysical prediction and cannot be used to study properties related to energy and dynamics.

### 3.4 Molecular Optimization and Generation

Efficient and effective molecular generation is of crucial importance in practice [236]. Especially, in the pharmaceutical industry, the discovery of new drugs is a long and expensive process that costs more than \$2.5 billion and 10–15 years on average [237]. Therefore, it is appealing to develop techniques that automatically and effectively generate plausible molecule candidates. The deep generative models, which learn to approximate the distribution of observed data, have been leveraged for molecule graph optimization and *de novo* generation [87, 238–242]. The optimization of the molecule usually starts with a hit compound and manipulates the graph to achieve better target properties like toxicity, drug-likeness, binding affinity, etc. The *de novo* molecule generative models generate novel molecules from scratch or conditioned on desired properties or specific fragments. In this case, molecule optimization can be considered as a conditional generation problem conditioned on the hit molecule. Thus, we review these two applications together in this section. There are two major frameworks in molecule graph generation: (1) fragment-based generative models and (2) molecule-based generative models [87, 243]. The fragment-based models generate molecule graph iteratively, where at each step the model choose an action, including adding, deleting, or editing one or multiple atoms, bonds, or functional groups. Such a fragment-based framework can be incorporated with reinforcement learning (DRL) that defines a Markov decision process (MDP) and learns the best generative policy by maximizing the expected accumulated rewards. It can also be implemented with autoregressive models like RNNs, which determine the action based on statuses at previous steps [244, 245]. The molecule-based model, on the other hand, generates all the attributes (i.e., atoms and bonds) of a molecule at once. Many generative methods equipped with GNNs fall into this category, including variational autoencoder (VAE) [246], generative adversarial network (GAN) [247], flow-based generative model [248], and score-based or diffusion generative model [249, 250]. VAE usually contains an encoder and a decoder that are trained to maximize the evidence lower bound concerning the log-likelihood of training data. GAN introduces two jointly trained components: a generator and a discriminator, where the generator generates samples while the discriminator attempts to distinguish between samples from the training data and those from the generator. Flow-based models are built upon a sequence of invertible operations that directly models the likelihood of the observed data. Score-based or diffusion model defines a Markov chain that adds random noise to data at each step and learns to denoise from the noise to recover the data. The following part in this section introduces molecule graph generative methods in detail.

**Metrics and Benchmarks** To measure the performance of deep generative models on molecule graphs, one needs to define comprehensive metrics and benchmarks [251, 252]. Simple but effective metrics include validity which assesses whether the generated molecules are valid, uniqueness/diversity which evaluates if a model generates a different molecule at each sampling, and novelty which measures whether generated molecules exist in the training set. Besides,

Preuer et al. propose the Fréchet ChemNet distance (FCD) [253] following the widely-used Fréchet Inception distance (FID) [254] in image synthesis, which is built upon the difference of hidden representations from ChemNet, a deep neural network, between generated molecules and those in the training set. Kullback-Leibler (KL) divergence is also used to measure whether the generative model approximates the distribution of the training set. In conditional generation or optimization, certain properties are used to evaluate the generative models. Many works build evaluation metrics on drug-likeness [255]. For example, the synthetic accessibility score (SAS) describes the ease of synthesis of molecules based on fragment contributions and a complexity penalty [256], the octanol-water partition coefficient  $\log P$  characterizes the drug-likeness of a molecule, the penalized  $\log P$  is the subtraction of original  $\log P$  and SAS, and quantitative estimate of drug-likeness (QED) applies desirability functions which provides a multicriteria metric to assess drug-likeness [257]. Maximum mean discrepancy (MMD) [258, 259] is another metric to evaluate the generated graphs. MMD is employed to measure the distribution difference between generated molecule graphs and training set on degrees, clustering coefficients, orbit counts, as well as bond lengths of different types. For candidate drug optimization or generative, the binding affinity of molecules with respect to the target protein pocket computed by molecular docking tools [260, 261] or molecular dynamic (MD) simulations [262–264] are also used as the objective [265, 266]. Energy-related properties, like HOMO-LUMO gap and dipole moment, have also been leveraged as the optimization or generation targets [267]. Additionally, Gao et al. [268] point out that sampling efficiency should be another important consideration in real molecular generation applications.

Several works have contributed to creating molecular generation benchmarks and databases. GuacaMol [251] by Brown et al. employ a standardized subset from ChEMBL database [117]. It includes validity, uniqueness, novelty, FCD, and KL divergence as the evaluation measurements. MOSES [252] by Polykovskiy et al. contains 1,936,962 molecular structures selected from ZINC [95] and is split into the training, test, and scaffold test sets containing approximately 1.6M, 176k, and 176k structure, respectively. Aside from the metrics included on GuacaMol, MOSES implements the similarity of fragments and scaffolds and properties distribution to evaluate the generative models. Besides, ZINC [95], ChEMBL [117], GDB databases [121, 269] are also used in training 2D molecule graph generative models. QM9 [122] which contains more than 130K 3D molecular structures, is also widely used for 3D molecular generation. Recently, GEOM [270] by Axelrod et al. introduces GEOM-QM9, an extension to QM9, containing multiple conformations for most molecules, and GEOM-Drugs containing 304,466 drug-like species up to a maximum of 91 heavy atoms.

**Fragment-based Generative Model** Fragment-based generative model modifies a molecule graph by adding, removing, or substituting a fragment (i.e., an atom or a motif) sequentially [271]. Such a framework can be directly modeled as an RL problem [265, 272–276]. At each time step  $t$ , an agent receives a reward

$r_t$  and predicts an action  $a_t \in \mathcal{A}$  given the current state  $s_t \in \mathcal{S}$ , and the next state  $s_{t+1} \in \mathcal{S}$  is depended solely on  $s_t$  and  $a_t$  following the MDP setting. Here,  $\mathcal{A}$  and  $\mathcal{S}$  denote the action and state space, respectively. In this case, the state is an incomplete molecule graph, the action is what fragment to add, remove, or substitute, and the agent is usually modeled by a deep neural network, including GNNs. Besides, the reward  $r_t$  evaluates how well the molecule is generated which could be a chemical metric or an output from property prediction ML models that approximate empirical measurements. The optimization objective of an RL agent (Equation 26) is to maximize the expected accumulated return  $R_t$  of a policy defined by the agent.

$$\mathbb{E}_\pi[R_t] = \mathbb{E}_\pi \left[ \sum_t^T \gamma^t r_t \right], \quad (26)$$

where  $\gamma \in (0, 1]$  is a discount rate and  $T$  is the maximal length of a trajectory. RL provides a generic framework for molecular design of different targets [277]. You and Liu et al. [278] propose a graph convolutional policy network (GCPN) that successively constructs a molecule by adding an atom, a substructure, or a bond, and is trained via the policy gradient algorithm. It built its agent on GCN [31]. Experiments show that GCPN can generate molecules with optimized or targeted penalized log  $P$  or QED properties. Jin et al. [279] present RationaleRL composed of rationale extraction, graph completion, and rationale distribution. RationaleRL is evaluated on GNK3 $\beta$  and JNK3 that measures the inhibition against glycogen synthase kinase-3 c-Jun N-terminal kinase-3 [280]. It also measures the validity, diversity, and novelty of the generative model. DeepGraphMol-Gen proposed by Khemchandani et al. [281] adapts GNNs for action prediction as well as property prediction in an RL setting. It designs a multi-objective reward function containing SAS, QED, and predicted binding affinity at the dopamine and norepinephrine transporters. Besides RL, autoregressive models can be incorporated with fragment-based molecule graph generation [244, 282]. GraphINVENT by Mercado et al. [282] leverages a tiered GNN architecture to generate a single bond at each step. Podda et al. [283] and Chen et al. [284] develop autoregressive generative models that operate on the fragments. Lim et al. [285] propose to extend a given molecule scaffold by sequentially adding nodes and edges, which guarantees the generated molecules preserve the certain scaffold. Xie et al. [286] propose a framework named MARS which combines molecule graph editing with MCMC sampling. The method employs a GNN to sample fragment-editing actions at each step adaptively. Shi et al. [287] introduce GraphAF built upon an autoregressive normalized flow-based generative model that adds nodes and edges to a molecule graph sequentially. GraphAF can also be fine-tuned with RL for molecular optimization of certain properties. Following the normalized flow model, GraphDF by Luo et al. [288] samples discrete latent variables which are mapped to additional nodes and edges via invertible modulo shift transforms.

Fragment-based generative models introduced so far have demonstrated the effectiveness of generating valid, unique, and diverse molecules as well as gen-

erating or optimizing towards desired SAS,  $\log P$ , and QED. However, these models only adapt 2D topological information without 3D geometric features. Many recent works have investigated generative models on 3D molecular structures as many properties, like energy and protein-ligand binding, are related to 3D geometries. Gebauer et al. [289] introduce G-SchNet, an autoregressive generative model for 3D molecular structure generation via placing atoms in 3D Euclidean space one by one. Gebauer et al. further introduce cG-SchNet [290], a conditional version of G-SchNet to generate molecules with certain motifs or low-energy (e.g., small HOMO-LUMO gap). Simm et al. [291] propose an RL formulation that adds atoms in 3D euclidean space sequentially and designs a reward function based on the fast quantum-chemical calculated electronic energy. The team also introduce MolGym, an RL environment comprising several molecular design tasks along with baseline models. Flam-Shepherd et al. [292] further introduce a 3D molecule generative RL framework to add fragments instead of single atoms at each step, which is more efficient in creating larger and complex molecules. Luo et al. [293] present G-SphereNet follows the flow-based generation while determining atoms in 3D space by predicting distances, angles, and torsion to preserve equivariance. Besides, researchers have investigated generating 3D molecules given a designated protein binding site. Docking scores along with other generic metrics are utilized to evaluate the deep generative models. Luo et al. [294] and GraphBP by Liu et al. [295] develop 3D autoregressive generative methods to sample the type and position of a new atom sequentially in the 3D binding pocket. Powers et al. [296] propose a molecular optimization method that expands a small fragment into a larger molecule within a protein site. At each step, a GNN trained by imitation learning selects the connecting point as well as the type and dihedral angle of a fragment to be connected. To preserve the equivariance in the 3D molecular generation, many works adopt a local spherical coordinate system in the generation process [289–291, 294, 295]. Besides, Imrie et al. [297] introduce DeLinker which generates linkers given two fragments in 3D Euclidean space.

**Molecule-based Generative model** Unlike fragment-based generative models, molecule-based generative models create the node features, edge features, and adjacency matrix of a molecule graph simultaneously. VAE, a popular generative model, has been leveraged for molecule-based generation [255, 298]. A VAE is composed of two sub-models: an encoder that encodes the input into a latent feature domain, and a decoder that maps the feature back to the input [246, 299]. The loss for training a VAE is given in Equation 27.

$$\ell = -\mathbb{E}_{z \sim q_\theta(z|x)} [\log p_\phi(x'|z)] + \text{KL}(q_\theta(z|x) \| p(z)), \quad (27)$$

where  $x$  is a input data,  $z$  is the latent vector,  $q_\theta$  is the encoder, and  $p_\phi$  is the decoder. The first term measures how well the model reconstructs the data and the second term regularizes the latent vector to be similar to a prior Gaussian distribution  $p(z)$  through a KL divergence. Such a framework has been leveraged to generate molecule graphs [299–301]. Simonovsky et al. [302] propose Graph-

VAE, where the encoder is modeled by a GNN and the decoder is modeled by an MLP that outputs the probability of node features, edge features, and adjacency matrix given the predefined number of nodes. The reconstruction loss measures the difference between generated and input molecule graphs in terms of node features, edge features, and adjacency matrix. Kwon et al. [303] improve the framework with an approximate graph matching for efficient reconstruction loss. Besides, the work incorporates RL and an auxiliary property prediction to improve molecule graph generation. Ma et al. [304] investigate regularized VAE to generate semantically valid molecule graphs. Constraints included in the decoder include atomic valence, graph connectivity, and node label compatibility. Bresson et al. [305] design a graph VAE with GCN [31] as the encoder and a novel two-step decoder. In the decoder, an MLP first predicts the molecular formula from the latent vector and then a GCN learns to place bonds between atoms from the same latent vector. Jin et al. [306] propose JT-VAE, a two-phase generative model employing subgraphs. JT-VAE first generates a junction tree (JT) representing the scaffold of chemical substructures and then the substructures are assembled into a complete molecule graph. Jin et al. [307] further improve the framework by leveraging larger and more flexible motifs and a decoder that operates in a hierarchical coarse-to-fine manner. The model demonstrates better performance in larger molecule generation compared to previous works. Li et al. [308] present DeepScaffold that generates molecules based on scaffolds. DeepScaffold contains DeepScaffold a VAE with a GNN encoder to complete atom and bond types for scaffold, a scaffold-based generator, and a filter for pharmacophore constraints. Mahmood et al. [309] also report masked molecular generation which learns the conditional distribution of unobserved atoms and bonds given observed components. VAE-based model can also be directly leveraged for conditional generation with respect to targeted properties [310–313]. Besides, given the learned latent representation by the VAE framework, molecular optimization can also be conducted in the latent space [314–318]. Jin et al. [319] report VJTNN, a molecular optimization framework based on JT-VAE, which includes stochastic latent codes to capture meaningful molecular variations. To avoid infeasible optimized molecules, the model introduces an adversarial training method to align the distribution of graphs on the latent domain. VJTNN achieves competitive performance on QED, penalized  $\log P$ , and biological activity optimization. LIMO, by Eckmann et al. [266], adapts VAE with an inceptionism-like reverse optimization to optimize generated molecules towards better binding affinity.

Apart from the VAE-based model, GAN has also been leveraged for molecule graph generation [320, 321]. GAN [247, 322–324] learns to approximate the distribution of actual data  $p_x(x)$  through a min-max game between a generator  $G$  and a discriminator  $D$ . The discriminator is trained to classify real samples from generated fake ones, while the generator learns to generate samples from random noise  $z \sim p_z(z)$  that the discriminator fails to recognize. The objective of GAN is given in Equation 28.

$$\min_G \max_D \left( \mathbb{E}_{x \sim p_x(x)} [\log D(x)] + \mathbb{E}_{z \sim p_z(z)} [\log(1 - D(G(z)))] \right), \quad (28)$$

where  $G$  attempts to generate plausible samples by minimizing the objective while  $D$  attempts to better detect fake samples by maximizing the objective. Cao et al. [325] implement the architecture of GAN to molecule graph generation and propose MolGAN. The generator in MolGAN generates an adjacency matrix and feature matrix that combine to define a molecule graph. Despite the generator and discriminator as in the standard GAN, MolGAN adapts an RL agent to generate molecules with targeted chemical properties (e.g., QED, SAS,  $\log P$ ). Maziarka et al. [326] introduce Mol-CycleGAN for molecular optimization, following CycleGAN [327]. Mol-CycleGAN generates a structurally similar molecule with preferred properties given a start compound. The model demonstrates effectiveness in optimizing penalized  $\log P$ . Tsujimoto et al. [328] further present L-MolGAN, which improves MolGAN performance on large molecule generation by penalizing the disconnected generated molecule graphs.

Other generative models have also been investigated for the molecule graph generation. The normalized flow-based model can also be leveraged in molecule-based generation besides fragment-based generation [329].

A flow-based model defines an invertible deterministic transformation  $f_\theta$  parameterized by  $\theta$  between the data space  $X$  and the latent space  $Z$  as  $f_\theta : Z \rightarrow X$  [248, 330].  $Z$  follows a prior Gaussian distribution  $p_Z$ , the log-likelihood of a data  $x$  is given in Equation 29.

$$\log p_X(x) = \log p_Z(f_\theta^{-1}(x)) + \log |\det J|, \quad (29)$$

where  $J = \frac{\partial f_\theta^{-1}(x)}{\partial x}$  is the Jacobian matrix of the function  $f_\theta^{-1}(x)$ . The objective of training a flow-based model is to maximize the log-likelihood. To efficiently compute  $\det J$ , the affine coupling mapping is leveraged in a normalized flow-based model [331, 332]. GraphNVP by Madhawa et al. [333] and MoFlow by Zang et al. [334] employ reversible normalizing flow-based model for the molecule graph generation. Both models decompose the generation into two phases, namely the generation of the adjacency matrix and node attributes, which yields the complete molecule graphs. Score-based [249, 335] or diffusion generative models [250, 336] are also investigated in molecule graph generation [337]. Song et al. [338] propose a unified framework that generalizes score-based or diffusion generative models through stochastic differential equations (SDEs). The forward diffusion process that transforms data  $x$  to a simple noise distribution is given in Equation 30.

$$dx = f(x, t)dt + g(t)dw, \quad (30)$$

where  $w$  is the standard Wiener process,  $f(\cdot, t)$  is the drift coefficient of  $x(t)$ , and  $g(\cdot)$  is the diffusion coefficient of  $x(t)$ . To sample data from random noise, the reversed SDE is given in Equation 31.

$$dx = [f(x, t) - g^2(t)\nabla_x \log p_t(x)]dt + g(t)d\tilde{w}, \quad (31)$$

where  $\tilde{w}$  is a standard Wiener process during the reversed flow. The training objective for a score function  $s_\theta(x, t)$  parameterized by  $\theta$  such that  $s_\theta(x, t) \approx$

$\nabla_x \log p_t(x)$  is given in Equation 32.

$$\mathbb{E}_{t \sim \mathcal{U}(0, T)} \mathbb{E}_{p_t(x)} [\lambda(t) \|\nabla_x \log p_t(x) - s_\theta(x)\|_2^2], \quad (32)$$

where  $\lambda(t)$  is a positive weighting function and  $\mathcal{U}(0, T)$  is a uniform distribution over the diffusion time interval. Hoogeboom et al. [267] propose equivariant diffusion model (EDM) which is built upon DDPM [250], a diffusion generative framework, to generate 3D molecules with an equivariant GNN model. EDM treats molecules as atomic types and coordinates without explicitly considering interatomic bonds. The framework has been demonstrated effective for random and conditional generation. Besides, diffusion model has been introduced to biomolecule generation (e.g., proteins) with GNNs [339].

**Molecular Conformation Generation** Despite molecular optimization and generation via GNN and deep generative models, another important application of generative models is molecular conformation generation, which aims at predicting the ensemble of low-energy 3D conformations of a molecule from its 2D graph solely [340, 341]. Understanding the low-energy conformations, the most stable configurations of molecules in 3D Euclidean space, is of great importance. Since 3D molecular structures determine the functions of chemical and biological processes [342]. Popular metrics for molecular conformation generation include the matching score (MAT) and the coverage score (COV) [343–345] which are both built up root-mean-square deviation (RMSD) computing the normalized Frobenius norm of the discrepancy of two aligned atomic coordinate systems [346]. Formally, let  $S_g$  denote the sets of generated conformations and  $S_r$  denote the one with reference conformations. The expression of MAT and COV are given in Equation 33 and 34, respectively.

$$\text{MAT}(S_g, S_r) = \frac{1}{|S_r|} \sum_{\mathbf{R} \in S_r} \min_{\hat{\mathbf{R}} \in S_g} \text{RMSD}(\mathbf{R}, \hat{\mathbf{R}}), \quad (33)$$

$$\text{COV}(S_g, S_r) = \frac{1}{|S_r|} |\{\mathbf{R} \in S_r | \text{RMSD}(\mathbf{R}, \hat{\mathbf{R}}) < \delta, \hat{\mathbf{R}} \in S_g\}|, \quad (34)$$

where  $\delta$  is a pre-defined threshold. Generally, a lower MAT score indicates a better accuracy and a higher COV score indicates a better diversity for the generative model. In many cases,  $\delta$  is set as 0.5 Å for QM9 and 1.25 Å for GEOM-Drugs. Ganea et al. [347] further propose recall metrics, MAT-R and COV-R, to measure the number of correctly predicted conformers, as well as the precision metrics, MAT-P and COV-P, to measure the number of generated structures of high quality.

Mansimov et al. [348] proposed to leverage a VAE framework with MPNN to directly predict the atomic coordinates from 2D graphs, which does not conserve the SE(3)-equivariance. To this end, the following works instead predict invariant geometric attributes like interatomic distances and torsional angles. Simm et al. [349] propose graph distance geometry (GraphDG) following the VAE framework to predict the interatomic distances. Conditional graph continuous

flow (CGCF) by Xu et al. [350] predicts the distance matrix via a flow-based model and optimizes generated conformations via a Markov chain Monte Carlo (MCMC) process and an energy-based tilting model (ETM). Both GraphDG and CGCF utilize the distance geometry (DG) method [351] to search atomic coordinates from the predicted distance matrix. ConfVAE by Xu et al. [352] improves the VAE pipeline which learns to encode molecule graphs into latent space and computes the 3D conformations as a principled bilevel optimization problem. However, these methods predict the distances and conformations separately where the errors in predicted distances accumulate in conformation calculations. In some cases, the predicted distance matrix may even fail to preserve valid 3D conformations. To avoid the issues caused by the two-stage strategy, ConfGF by Shi et al. [344] and DGSM by Luo et al. [353] directly estimates the gradient fields of the logarithm density of atomic coordinates (pseudo force fields) via a score-based generative method. The former relies on static molecule graphs to predict conformations as previous methods, while the latter deploys a dynamic graph construction that better models long-range interactions. Further, GeoDiff by Xu et al. [345] leverages the denoising diffusion probabilistic model (DDPM), a diffusion generative model, to generate 3D conformations via reversing a diffusion process. To keep the  $SE(3)$ -equivariance, ConfGF, DGSM, and GeoDiff leverage equivariant GNNs to make predictions of atomic coordinates. Besides interatomic distances and atomic positions, recent works have investigated to predict torsional angles in conformation generation. Ganea et al. propose GeoMol [347] which predicts local 3D structures and ensembles the local structures by predicting the torsion angles. Jing et al. [354] introduce torsional diffusion, a diffusion generative model that formalizes molecular conformation generation in the space of torsional angles. TorsionNet by Gogineni et al. [355] presents the conformation generation as a reinforcement learning problem to sample torsion at each time step.

In summary, various generative models, including VAE, GAN, flow-based model, and score-based/diffusion model, have been implemented for a molecular generation. The fragment-based generation defines the generative process as sequentially adding atoms, bonds, or motifs to build the graph. Such a framework, incorporated with RL or autoregressive models, makes the process tractable. RL provides a suitable framework for molecular optimization. Recently works that utilize a flow-based model to generate molecules autoregressively have also been a success. The molecule-based generation, on the other hand, generates the whole molecule simultaneously. Within this category, VAE-based generative models are widely used and explicitly learn a meaningful latent space where molecular search and optimization can be easily conducted. A few works leverage GAN models for molecular generation, however, it is not as widely used as VAE, due to potentially unstable training and hard to manipulate the generation. Flow-based models can also be leveraged for the molecule-based generation which generates node features, bond features, and/or adjacency matrices simultaneously. Recently, the development of score-based or diffusion models in image generation has also inspired works in molecular generation. Moreover, recent re-

search is paying more attention to 3D molecular structure generations beyond 2D graphs. Since 3D structures play an essential role in various molecular applications. Notably, there are also massive works that build molecular generative models on string-based representations (e.g., SMILES) [255, 356–358]. However, this is not the focus of this chapter, and compared to string-based representations, molecule graph generation with GNNs provides more topological and geometric information that is vital in molecular science.

### 3.5 Others

**Synthesis Planning and Retrosynthesis Prediction** Synthesis planning aims at determining the synthesis path of a chemical compound from available starting materials through a series of chemical reactions [359]. Retrosynthetic prediction, formalized by E. J. Corey [360], refers to the reverse problem: to select suitable disconnections recursively given the desired product [361]. The major challenge in the computational retrosynthetic analysis is the combinatorial exploration space of chemical reactions for target compounds. There are two major approaches: template-based and template-free methods. The former matches the target molecule to chemical reaction rules to yield one or multiple candidate precursors. The latter directly predicts the reactants from target products. Recently, several works have investigated template-free or semi template-free retrosynthesis prediction via GNNs. USPTO-50k [362] which contains 50k atom-mapped reactions with 10 reaction classes is the most widely used benchmark. G2G proposed by Shi et al. [363] learns to translate a target molecule into a set of reactant molecule graphs. G2G contains two steps: (1) edit prediction that splits the target molecule into multiple synthons via predicting the reaction centers, and (2) synthon completion that transforms the synthons into reactant graphs. Such a workflow has been leveraged by many works. Sun et al. [364] propose to formalize such a retrosynthesis prediction problem as an energy-based model (EBM). Somnath et al. [365] introduce leaving graphs from a precomputed vocabulary for synthon completion, which greatly reduces the complexity of synthon generation. Lin et al. [366] further present G2GT, which leverages recent graph transformer (i.e., Graphomer [42]) in template-free retrosynthesis prediction. Han et al. [367] propose GNN-Retro that combines GNN with the A\* search algorithm. Besides retrosynthetic prediction, GNNs have been implemented other tasks concerning chemical reactions, including predicting reaction products [368, 369], reaction conditions [370], reaction yields [371, 372], and synthesizability [373–375].

**Molecular Knowledge Graph** Knowledge graphs (KGs) are graphical structured knowledge bases where each node models a knowledge entity and each edge models the relations between entities [7, 376, 377]. KGs are a powerful tool that incorporates multiple data sources. In molecular science, KGs have been leveraged to represent biomedical knowledge. Specifically, nodes may model various entities, including drugs, protein targets, diseases, side effects, pathways,

etc. Such biomedical KGs can be leveraged to predict drug-drug interactions (DDIs), which aims at predicting the outcomes of combined use of two or more drugs, like side effects, adverse reactions, or even toxicity [378–382]. Sources of DDI knowledge include DrugBank [168, 383], KEGG [384, 385], BioSNAP [386], PharmGKB [387, 388], Bio2RDF [7, 389], etc. In DDI KG, nodes model drugs and edges model interactions, thus DDI prediction can be treated as link prediction tasks. GNNs have since made progress on DDI prediction based on KGs. Feng et al. [390] implement GCN [31] on drug-drug interaction KG to predict potential DDIs. Yu et al. [391] introduce SumGNN which utilizes a local subgraph in KG around drug pairs instead of the entire KG to obtain information. Multiple works investigate leveraging multi-modal data to enhance DDI predictions [392, 393]. Lyu et al. [394] propose MDNN containing KG and heterogeneous pathways to obtain multi-modal representations. Lin et al. [395] propose an end-to-end framework built upon GNNs which captures potential neighborhoods of drugs by leveraging their relations in KG. Zhang et al. [396] propose MKGE which combines KG embedding with molecular structure features for DDI predictions. He et al. [397] propose to fuse the topological information from molecular graphs and the interaction information in the form of SMILES. Some works directly build GNNs on molecular graphs of drug pairs to predict DDIs [398–400] instead of relying on KGs. Besides DDI KGs, other KGs have also been investigated like protein-protein interaction KGs [56, 401–403] and chemical reaction networks [404]. Zitnik et al. [405] propose Decagon based on graph autoencoder to predict side effects of drug pairs and build a large multi-modal KG including protein-protein, drug-protein, and drug-drug interactions.

**Biomolecules** Though the focus of this chapter lies in small organic molecules. It is worth mentioning that GNNs have also been leveraged to learn expressive representations of large biomolecules (i.e., proteins, RNAs, DNAs, etc.). AlphaFold [406], which is a milestone in protein structure prediction, utilizes attention and message-passing mechanisms. Following this, multiple works have probed improving protein structure prediction from amino acid sequences [407–410]. Many works have also developed GNN-based models in various protein applications, including protein function prediction [411–413], protein-compound interactions [414–417] and protein design [339, 418–421]. Besides proteins, several works have investigated RNAs and DNAs via GNNs [422–424].

## 4 Self-supervised Learning on Molecule Graphs

The previous section reviews various GNN architectures with expressive message-passing operations for molecular systems. However, a well-designed neural network does not guarantee to perform well, as the performance of the model is also closely related to the quantity and quality of data. In supervised learning, the ML models require instance-label pairs to learn representations. Labeling data can be expensive and time-consuming, and acquiring labels in molecular science takes even more effort. Measuring the attributes and properties of

molecules depends on complicated wet-lab experiments and/or expensive simulations. Thus, labeled molecular data is far from sufficient in many applications. Besides, molecular labels are usually noisy since different experimental or simulation environments can lead to significant fluctuations. Moreover, the chemical space of potential molecules is magnificent. The number of potential pharmaco logically active molecules is estimated to be in the order of  $10^{23}$  to  $10^{60}$  [425]. For the GNN trained on limited and noisy data in a supervised learning manner, it is of great challenge to generalize novel molecules from the huge chemical space. Despite the limited labeled molecular data, the number of molecules in publicly available databases is growing fast in recent years. Such databases include ZINC [95], PubChem [114], Enamine REAL library, etc. A question may be asked: can one make use of the large unlabeled data to improve ML models?

Following the insight, self-supervised learning (SSL) [426, 427] is proposed to utilize the large unlabelled data and learn better representations that are generalizable to various challenging applications. As the name indicates, SSL trains the ML models via the supervisory signals from the data itself, which usually utilizes the underlying structure in the data. There are two major categories of SSL: (1) non-contrastive learning methods, (2) contrastive learning methods. Many non-contrastive learning methods rely on generative models that learn meaningful representations by recovering the data from partially observed input. Examples in computer vision include colorization of grayscaled images [428], prediction of rotation of images [429], and reconstruction of partially masked image [430–433]. In natural language processing (NLP), self-supervised pre-training via prediction of masked tokens has been a standard technique in deploying large language models [434, 435]. On the other hand, contrastive learning (CL) methods, like MoCo [436], SimCLR [437], and SwAV [438], learns representations by attracting the representations of the positive pairs together and pushing representations of the negative pairs away, where positive pairs are perturbed instances from the same data while negative samples are instances from different data [439]. For a query representation  $\mathbf{q}$  and a batch of  $N + 1$  keys containing only one key  $\mathbf{k}_+$  from a positive instance, the information noise-contrastive estimation (InfoNCE) loss, a popular type of contrastive loss, is given in Equation 35.

$$\ell = -\log \frac{\exp((\mathbf{q}^\top \mathbf{k}_+)/\tau)}{\sum_{i=0}^N \exp((\mathbf{q}^\top \mathbf{k}_i)/\tau)}, \quad (35)$$

where  $\tau$  is the temperature parameter. Such a loss can be considered as a  $(N+1)$ -way classifier to classify  $\mathbf{q}$  as its positive instance  $\mathbf{k}_+$ . CL has been a success in a wide variety applications [440–444]. Following the objective of contrasting representation in CL, researchers design non-contrastive methods that only require pulling together representations of positive pairs, like BYOL [445], SimSiam [446], Barlow Twins [447], and VICReg [448], which simply the framework.

Since proposed, SSL has been introduced to learning molecular representations from large unlabeled data with GNNs [449]. As shown in Figure 4, SSL on molecule graphs has two steps. In the pre-training step, the GNN is trained on large unlabeled molecular data via self-supervised learning tasks, where the

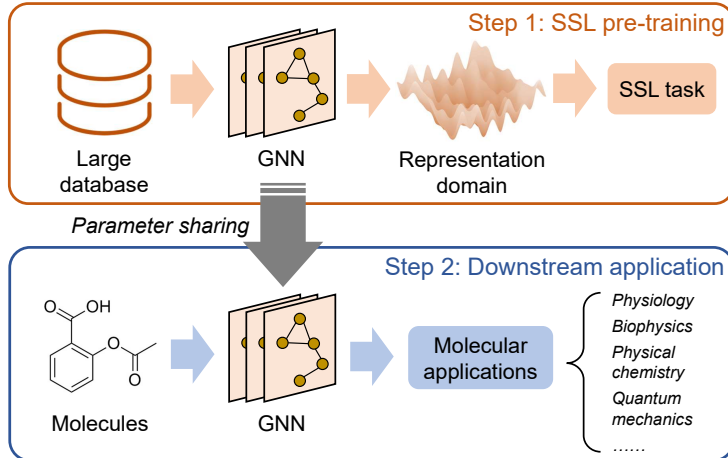


**Fig. 4.** Illustration of self-supervised learning pre-training and fine-tuning on downstream tasks.

GNN parameters are optimized to encode expressive molecular representations. In the downstream application step, the pre-trained GNN is fine-tuned or used to directly extract the learned representations for various molecular applications. By this means, the GNN model digs into the molecule graphs and learns better representations that can perform well even on tasks with noisy and limited data. The following paragraphs will enumerate works that investigate different SSL techniques on molecule graphs.

Non-contrastive SSL methods are first introduced to learn representations from 2D molecule graphs. Most of such molecular SSL methods are based on predicting the probability or attribute of a masked or partially observed substructure occurring within a molecule [450]. Hu et al. [56] introduce pre-training tasks at the levels of both individual nodes and the whole graphs. The node-level pre-training contains two self-supervised tasks: context prediction which uses subgraphs to predict their surrounding graph structures, and masked attribute prediction which pre-trains GNNs through predicting the attributes of masked nodes/edges. While the graph-level pre-training is based on supervised learning of domain-specific graph labels, which is still constrained by the availability of molecular labels. Rong et al. [59] further introduce contextual property prediction which predicts masked subgraphs and graph-level motif prediction which predicts the containing functional groups within a molecule as two SSL tasks. This work also adapts a transformer-based model to learn representations from molecule graphs. Zhang et al. [451] also design motif-level self-supervised tasks that leverage the BRICS algorithm to construct motif trees and pre-trains GNNs by generating molecular graphs motif-by-motif. At each step of pre-training, the model first predicts the topology which determines whether a node has extra motifs to be connected to, and then predicts the motif label from motif vocabulary.

He et al. [452] extends the idea of predicting masked attributes even further by leveraging information in chemical reactions. The work named masked molecule modeling (MMM) adapts Graphomer [42] to take in molecule graphs in a chemical reaction, the GNN model is then trained to reconstruct randomly masked atoms, motifs, and bonds within the reaction. Besides, Liu et al. [453] leverage N-gram graph representations to embed molecule graphs in an unsupervised manner that assembles the node features in short walks. The graph embedding method requires no training and can be used for different ML models. Sun et al. [454] introduce InfoGraphn which learns presentations by maximizing the mutual information between the graph-level embedding and multi-level substructure embedding.

Apart from 2D graphs, recent works have probed SSL strategies to include 3D geometric information. To acquire 3D conformations for pre-training, some works [67, 455, 456] use efficient Merck molecular force field (MMFF94) function in RDKit <sup>2</sup> to simulate 3D atomic positions. While other methods [457–461] leverage datasets containing 3D molecular conformations at equilibrium calculated by more precise yet expensive density functional theory (DFT), including QM9, GEOM, PCQM4Mv2, and Molecule3D. Chen et al. [462] design an algebraic graph-assisted bidirectional transformer method that fuses representations from the algebraic graph and transformer. The algebraic graph embeds 3D stereochemical information into graph invariants and the bidirectional transformer embeds representations from SMILES [51] language. The fused representations can be incorporated with a variety of machine learning algorithms, including tree-based models and DNNs, for various molecular property predictions. Fang et al. [67] propose a geometry-enhanced molecular representation learning method (GEM) that learns representations through predicting bond lengths, bond angles, and interatomic distances. It also introduces an auxiliary graph-level SSL task that predicts molecular fingerprints, i.e., ECFP and MACCS keys. Zhou et al. [456] present masked atom prediction and 3D position denoising including pair-distance prediction and direct coordinate prediction in the framework named Uni-Mol. The input molecule is perturbed by masking some atoms and adding noise to 3D coordinates randomly. Uni-Mol also adapts a transformer-based model with invariant spatial positional encoding to embed geometric information. With the recent development of equivariant GNNs on 3D molecules, researchers have explored SSL strategies that perform to improve the expressiveness of such models. Zaidi et al. [459], Liu et al. [460], and Jiao et al. [461] have demonstrated the effectiveness of position denoising as self-supervised pre-training on equivariant GNNs. The three works share the similar idea that adds noise to the 3D atomic positions at equilibrium and let the GNN predict the noise [459, 461], or predict the original interatomic distances [460]. They have also shown that the positional denoising SSL objective is equivalent to the force field prediction from equilibrium structures. This sheds a light on leveraging equivariant GNNs for a wider range of applications like predicting potential energy surfaces and molecular dynamics simulations.

<sup>2</sup> <https://www.rdkit.org/>

Inspired by the success of CL, CL-based self-supervised methods have been introduced to molecular systems. Wang et al. [100] propose MolCLR, a CL framework for molecular representation learning with GNNs. To create contrastive pairs, MolCLR implements three molecule graph augmentation strategies: atom masking, bond deletion, and subgraph removal. A positive pair contains graphs augmented from the molecule while a negative pair contains those augmented from different molecules. MolCLR adapts the normalized temperature-scaled cross entropy (NT-Xent) loss from SimCLR [437], which is a modification of the InfoNCE loss. Given a batch of  $N$  molecules, each molecule generates two augmented graphs, and the NT-Xent loss for a positive pair  $(i, j)$  in the batch of  $2N$  graphs is given in Equation 36.

$$\ell_{i,j} = -\log \frac{\exp((\mathbf{z}_i^\top \mathbf{z}_j)/\tau)}{\sum_{k=1}^{2N} \mathbb{1}_{\{k \neq i\}} \exp((\mathbf{z}_i^\top \mathbf{z}_k)/\tau)}, \quad (36)$$

where  $\mathbb{1}_{\{\cdot\}}$  is an indicator function, and  $\mathbf{z}_i, \mathbf{z}_j$  are normalized representations of the positive pair. Zhang et al. [463] further propose MICRO-Graph which extracts informative subgraphs from molecules via GNNs and performs contrastive pre-training on sampled subgraphs learned by GNNs. Similar to non-contrastive learning methods, CL has also gone beyond 2D molecule graphs and applies multi-view CL pre-training. Liu et al. [457], Stärk et al. [458], and Li et al. [455] propose GraphMVP, 3D infomax, and GeomGCL, respectively. All three methods conduct contrastive pre-training between 2D topological graphs and 3D geometric structures to learn molecular representations with 3D information embedded. Namely, 2D and 3D views from a molecule compose a positive pair while others are negative pairs. GraphMVP also utilizes a generative model in the representation domain as an auxiliary SSL task. Besides, Zhu et al. [464] develop a dual-view CL framework that contrasts between SMILES strings and 2D molecule graphs, where the former is encoded by a transformer and the latter is encoded by GNN. Further, MEMO from Zhu et al. [465] presents a multi-view CL that leverages four molecular representations, including 2D topology, 3D geometry, SMILES string, and fingerprint. Some works have sought to fuse chemical domain knowledge in molecular CL models to learn better representations. Following the insight, Wang et al. [466] introduce iMolCLR to improve previous CL frameworks in two aspects: (1) mitigating faulty negative instances via considering molecular similarities in NT-Xent loss, and (2) fragment-level contrasting between substructures decomposed via the BRICS algorithm. Fang et al. [467] propose a molecule cluster strategy that utilizes functional groups and fingerprints similarity to select similar molecules as positive pairs and dissimilar molecules as negative pairs in contrastive training. The work also includes functional group embeddings as an input to GNN. MoCL by Sun et al. [468] leverages local-level and global-level in contrastive learning on molecule graphs. Specifically, the local-level domain knowledge augments the molecule graph by replacing a substructure with a bioisostere which perturbs the instance while maintaining the chemical properties. The global-level domain knowledge introduces a loss that minimizes the difference between the similarity of learned representations

and ECFP similarity between two molecules. Fang et al. [469] propose knowledge-enhanced CL that includes graph augmentations based on the chemical element knowledge graph as well as the know-aware message-passing functions. In another model named CoSP, Gao et al., [470] leverage information besides small organic molecules to learn better representations. CoSP adapts a cross-domain CL framework that generates contrastive pairs from ligand molecules and protein binding pockets. It also introduces ChemInfoNCE loss to reduce the negative sampling bias through a chemical similarity-enhanced negative ligand sampling strategy.

## 5 Conclusion

Recent years have witnessed an immense growth of graph neural networks in molecular sciences. In this survey, we review the generic message-passing framework for building graph neural networks. Graph neural network architectures designed for small organic molecules are introduced. Works on learning representations from 2D topological graphs as well as recent efforts in leveraging 3D geometric information are covered. Also, we try to provide a comprehensive overview of benchmarks, metrics, and graph neural network models in various molecular applications, including property predictions, molecular scoring, and docking, molecular optimization and generation, molecular dynamics, synthesis planning, molecular knowledge graph, etc. The last section epitomizes molecular self-supervised learning with graph neural networks. Graph neural networks have been successfully implemented to solve a wide variety of molecular tasks. However, the acquisition of high-quality labeled molecular data is still expensive and time-consuming. One direction that is worth exploring is to introduce domain knowledge to molecular graph neural networks for solving challenging problems with limited or noisy data.

## References

1. Bronstein, M. M., Bruna, J., LeCun, Y., Szlam, A. & Vandergheynst, P. Geometric deep learning: going beyond euclidean data. *IEEE Signal Processing Magazine* **34**, 18–42 (2017).
2. Dai, H., Kozareva, Z., Dai, B., Smola, A. & Song, L. *Learning steady-states of iterative algorithms over graphs* in *International conference on machine learning* (2018), 1106–1114.
3. Fan, W., Ma, Y., Li, Q., He, Y., Zhao, E., Tang, J. & Yin, D. *Graph neural networks for social recommendation* in *The world wide web conference* (2019), 417–426.
4. Wu, Y., Lian, D., Xu, Y., Wu, L. & Chen, E. *Graph convolutional networks with markov random field reasoning for social spammer detection* in *Proceedings of the AAAI conference on artificial intelligence* **34** (2020), 1054–1061.

5. Duvenaud, D. K., Maclaurin, D., Iparraguirre, J., Bombarell, R., Hirzel, T., Aspuru-Guzik, A. & Adams, R. P. Convolutional networks on graphs for learning molecular fingerprints. *Advances in neural information processing systems* **28** (2015).
6. Kearnes, S., McCloskey, K., Berndl, M., Pande, V. & Riley, P. Molecular graph convolutions: moving beyond fingerprints. *Journal of computer-aided molecular design* **30**, 595–608 (2016).
7. Dumontier, M., Callahan, A., Cruz-Toledo, J., Ansell, P., Emonet, V., Belleau, F. & Droit, A. *Bio2RDF release 3: a larger connected network of linked data for the life sciences* in *Proceedings of the 2014 International Conference on Posters & Demonstrations Track* **1272** (2014), 401–404.
8. Hamaguchi, T., Oiwa, H., Shimbo, M. & Matsumoto, Y. Knowledge transfer for out-of-knowledge-base entities: A graph neural network approach. *arXiv preprint arXiv:1706.05674* (2017).
9. Sanchez-Gonzalez, A., Heess, N., Springenberg, J. T., Merel, J., Riedmiller, M., Hadsell, R. & Battaglia, P. *Graph networks as learnable physics engines for inference and control* in *International Conference on Machine Learning* (2018), 4470–4479.
10. Thomas, N., Smidt, T., Kearnes, S., Yang, L., Li, L., Kohlhoff, K. & Riley, P. Tensor field networks: Rotation-and translation-equivariant neural networks for 3d point clouds. *arXiv preprint arXiv:1802.08219* (2018).
11. Fout, A., Byrd, J., Shariat, B. & Ben-Hur, A. Protein interface prediction using graph convolutional networks. *Advances in neural information processing systems* **30** (2017).
12. Qi, X., Liao, R., Jia, J., Fidler, S. & Urtasun, R. *3d graph neural networks for rgbd semantic segmentation* in *Proceedings of the IEEE International Conference on Computer Vision* (2017), 5199–5208.
13. Wang, T., Liao, R., Ba, J. & Fidler, S. *Nervenet: Learning structured policy with graph neural networks* in *International conference on learning representations* (2018).
14. LeCun, Y., Bengio, Y. & Hinton, G. Deep learning. *Nature* **521**, 436–444 (2015).
15. Zhou, J., Cui, G., Hu, S., Zhang, Z., Yang, C., Liu, Z., Wang, L., Li, C. & Sun, M. Graph neural networks: A review of methods and applications. *AI Open* **1**, 57–81 (2020).
16. Wu, Z., Pan, S., Chen, F., Long, G., Zhang, C. & Philip, S. Y. A comprehensive survey on graph neural networks. *IEEE transactions on neural networks and learning systems* **32**, 4–24 (2020).
17. Krizhevsky, A., Sutskever, I. & Hinton, G. E. Imagenet classification with deep convolutional neural networks. *Advances in neural information processing systems* **25** (2012).
18. He, K., Zhang, X., Ren, S. & Sun, J. *Deep residual learning for image recognition* in *Proceedings of the IEEE conference on computer vision and pattern recognition* (2016), 770–778.

19. Hochreiter, S. & Schmidhuber, J. Long short-term memory. *Neural computation* **9**, 1735–1780 (1997).
20. Chami, I., Abu-El-Haija, S., Perozzi, B., Ré, C. & Murphy, K. Machine learning on graphs: A model and comprehensive taxonomy. *arXiv preprint arXiv:2005.03675*, 1 (2020).
21. You, J., Ying, Z. & Leskovec, J. Design space for graph neural networks. *Advances in Neural Information Processing Systems* **33**, 17009–17021 (2020).
22. Gilmer, J., Schoenholz, S. S., Riley, P. F., Vinyals, O. & Dahl, G. E. Neural message passing for quantum chemistry in *International conference on machine learning* (2017), 1263–1272.
23. Battaglia, P. W., Hamrick, J. B., Bapst, V., Sanchez-Gonzalez, A., Zambaldi, V., Malinowski, M., Tacchetti, A., Raposo, D., Santoro, A., Faulkner, R., *et al.* Relational inductive biases, deep learning, and graph networks. *arXiv preprint arXiv:1806.01261* (2018).
24. Shuman, D. I., Narang, S. K., Frossard, P., Ortega, A. & Vandergheynst, P. The emerging field of signal processing on graphs: Extending high-dimensional data analysis to networks and other irregular domains. *IEEE signal processing magazine* **30**, 83–98 (2013).
25. Li, Y., Tarlow, D., Brockschmidt, M. & Zemel, R. *Gated graph sequence neural networks* in (2016).
26. Battaglia, P., Pascanu, R., Lai, M., Jimenez Rezende, D., *et al.* Interaction networks for learning about objects, relations and physics. *Advances in neural information processing systems* **29** (2016).
27. Gao, H., Wang, Z. & Ji, S. *Large-scale learnable graph convolutional networks* in *Proceedings of the 24th ACM SIGKDD international conference on knowledge discovery & data mining* (2018), 1416–1424.
28. Zhang, J., Shi, X., Xie, J., Ma, H., King, I. & Yeung, D.-Y. Gaan: Gated attention networks for learning on large and spatiotemporal graphs. *arXiv preprint arXiv:1803.07294* (2018).
29. Bruna, J., Zaremba, W., Szlam, A. & LeCun, Y. Spectral networks and locally connected networks on graphs. *arXiv preprint arXiv:1312.6203* (2013).
30. Defferrard, M., Bresson, X. & Vandergheynst, P. Convolutional neural networks on graphs with fast localized spectral filtering. *Advances in neural information processing systems* **29** (2016).
31. Kipf, T. N. & Welling, M. *Semi-Supervised Classification with Graph Convolutional Networks* in *Proceedings of the International Conference on Learning Representations* (2017).
32. Maas, A. L., Hannun, A. Y. & Ng, A. Y. Rectifier nonlinearities improve neural network acoustic models in *Proceedings of Machine Learning Research* **30** (2013), 3.
33. Hamilton, W., Ying, Z. & Leskovec, J. Inductive representation learning on large graphs. *Advances in neural information processing systems* **30** (2017).

34. Xu, K., Hu, W., Leskovec, J. & Jegelka, S. *How Powerful are Graph Neural Networks?* in *International Conference on Learning Representations* (2019).
35. Veličković, P., Cucurull, G., Casanova, A., Romero, A., Lio, P. & Bengio, Y. Graph attention networks. *arXiv preprint arXiv:1710.10903* (2017).
36. Cho, K., Van Merriënboer, B., Gulcehre, C., Bahdanau, D., Bougares, F., Schwenk, H. & Bengio, Y. Learning phrase representations using RNN encoder-decoder for statistical machine translation. *arXiv preprint arXiv:1406.1078* (2014).
37. Tai, K. S., Socher, R. & Manning, C. D. Improved semantic representations from tree-structured long short-term memory networks. *arXiv preprint arXiv:1503.00075* (2015).
38. Peng, N., Poon, H., Quirk, C., Toutanova, K. & Yih, W.-t. Cross-sentence n-ary relation extraction with graph lstms. *Transactions of the Association for Computational Linguistics* **5**, 101–115 (2017).
39. Zayats, V. & Ostendorf, M. Conversation modeling on Reddit using a graph-structured LSTM. *Transactions of the Association for Computational Linguistics* **6**, 121–132 (2018).
40. Rampášek, L., Galkin, M., Dwivedi, V. P., Luu, A. T., Wolf, G. & Beaini, D. Recipe for a General, Powerful, Scalable Graph Transformer. *arXiv preprint arXiv:2205.12454* (2022).
41. Vaswani, A., Shazeer, N., Parmar, N., Uszkoreit, J., Jones, L., Gomez, A. N., Kaiser, Ł. & Polosukhin, I. Attention is all you need. *Advances in neural information processing systems* **30** (2017).
42. Ying, C., Cai, T., Luo, S., Zheng, S., Ke, G., He, D., Shen, Y. & Liu, T.-Y. Do transformers really perform badly for graph representation? *Advances in Neural Information Processing Systems* **34**, 28877–28888 (2021).
43. Dwivedi, V. P. & Bresson, X. A generalization of transformer networks to graphs. *arXiv preprint arXiv:2012.09699* (2020).
44. Kim, J., Nguyen, T. D., Min, S., Cho, S., Lee, M., Lee, H. & Hong, S. Pure Transformers are Powerful Graph Learners. *arXiv preprint arXiv:2207.02505* (2022).
45. Choromanski, K., Likhoshesterov, V., Dohan, D., Song, X., Gane, A., Sarlos, T., Hawkins, P., Davis, J., Mohiuddin, A., Kaiser, Ł., *et al.* Rethinking attention with performers. *arXiv preprint arXiv:2009.14794* (2020).
46. Vinyals, O., Bengio, S. & Kudlur, M. Order matters: Sequence to sequence for sets. *arXiv preprint arXiv:1511.06391* (2015).
47. Zhang, M., Cui, Z., Neumann, M. & Chen, Y. *An end-to-end deep learning architecture for graph classification* in *Proceedings of the AAAI conference on artificial intelligence* **32** (2018).
48. Ying, Z., You, J., Morris, C., Ren, X., Hamilton, W. & Leskovec, J. Hierarchical graph representation learning with differentiable pooling. *Advances in neural information processing systems* **31** (2018).
49. Lee, J., Lee, I. & Kang, J. *Self-attention graph pooling* in *International conference on machine learning* (2019), 3734–3743.

50. Atz, K., Grisoni, F. & Schneider, G. Geometric deep learning on molecular representations. *Nature Machine Intelligence* **3**, 1023–1032 (2021).
51. Weininger, D. SMILES, a chemical language and information system. 1. Introduction to methodology and encoding rules. *Journal of chemical information and computer sciences* **28**, 31–36 (1988).
52. SMARTS - a language for describing molecular patterns Date access July 30, 2022. <https://www.daylight.com/dayhtml/doc/theory/theory.smarts.html>.
53. Krenn, M., Häse, F., Nigam, A., Friederich, P. & Aspuru-Guzik, A. Self-referencing embedded strings (SELFIES): A 100% robust molecular string representation. *Machine Learning: Science and Technology* **1**, 045024 (2020).
54. Rogers, D. & Hahn, M. Extended-connectivity fingerprints. *Journal of chemical information and modeling* **50**, 742–754 (2010).
55. Durant, J. L., Leland, B. A., Henry, D. R. & Nourse, J. G. Reoptimization of MDL keys for use in drug discovery. *Journal of chemical information and computer sciences* **42**, 1273–1280 (2002).
56. Hu, W., Liu, B., Gomes, J., Zitnik, M., Liang, P., Pande, V. & Leskovec, J. *Strategies for Pre-training Graph Neural Networks* in *International Conference on Learning Representations* (2020).
57. Yang, K., Swanson, K., Jin, W., Coley, C., Eiden, P., Gao, H., Guzman-Perez, A., Hopper, T., Kelley, B., Mathea, M., *et al.* Analyzing learned molecular representations for property prediction. *Journal of chemical information and modeling* **59**, 3370–3388 (2019).
58. Xiong, Z., Wang, D., Liu, X., Zhong, F., Wan, X., Li, X., Li, Z., Luo, X., Chen, K., Jiang, H., *et al.* Pushing the boundaries of molecular representation for drug discovery with the graph attention mechanism. *Journal of medicinal chemistry* **63**, 8749–8760 (2019).
59. Rong, Y., Bian, Y., Xu, T., Xie, W., WEI, Y., Huang, W. & Huang, J. *Self-Supervised Graph Transformer on Large-Scale Molecular Data* in *Advances in Neural Information Processing Systems* **33** (2020), 12559–12571.
60. Han, J., Rong, Y., Xu, T. & Huang, W. Geometrically equivariant graph neural networks: A survey. *arXiv preprint arXiv:2202.07230* (2022).
61. Blanco-Claraco, J. L. A tutorial on SE(3) transformation parameterizations and on-manifold optimization. *arXiv preprint arXiv:2103.15980* (2021).
62. Schütt, K. T., Arbabzadah, F., Chmiela, S., Müller, K. R. & Tkatchenko, A. Quantum-chemical insights from deep tensor neural networks. *Nature communications* **8**, 1–8 (2017).
63. Schütt, K., Kindermans, P.-J., Sauceda Felix, H. E., Chmiela, S., Tkatchenko, A. & Müller, K.-R. Schnet: A continuous-filter convolutional neural network for modeling quantum interactions. *Advances in neural information processing systems* **30** (2017).

64. Unke, O. T. & Meuwly, M. PhysNet: A neural network for predicting energies, forces, dipole moments, and partial charges. *Journal of chemical theory and computation* **15**, 3678–3693 (2019).
65. Gasteiger, J., Groß, J. & Günnemann, S. *Directional message passing for molecular graphs* in *International Conference on Learning Representations* (2019).
66. Klicpera, J., Giri, S., Margraf, J. T. & Günnemann, S. Fast and uncertainty-aware directional message passing for non-equilibrium molecules. *arXiv preprint arXiv:2011.14115* (2020).
67. Fang, X., Liu, L., Lei, J., He, D., Zhang, S., Zhou, J., Wang, F., Wu, H. & Wang, H. Geometry-enhanced molecular representation learning for property prediction. *Nature Machine Intelligence* **4**, 127–134 (2022).
68. Adams, K., Pattanaik, L. & Coley, C. W. Learning 3D Representations of Molecular Chirality with Invariance to Bond Rotations. *arXiv preprint arXiv:2110.04383* (2021).
69. Gilmore, R. *Lie Groups, Physics, and Geometry: An Introduction for Physicists, Engineers and Chemists* (Cambridge University Press, 2008).
70. Fuchs, F., Worrall, D., Fischer, V. & Welling, M. Se (3)-transformers: 3d roto-translation equivariant attention networks. *Advances in Neural Information Processing Systems* **33**, 1970–1981 (2020).
71. Brandstetter, J., Hesselink, R., van der Pol, E., Bekkers, E. J. & Welling, M. *Geometric and Physical Quantities improve E(3) Equivariant Message Passing* in *International Conference on Learning Representations* (2022).
72. Anderson, B., Hy, T.-S. & Kondor, R. *Cormorant: Covariant Molecular Neural Networks* 2019. <https://arxiv.org/abs/1906.04015>.
73. Schütt, K. T., Unke, O. T. & Gastegger, M. *Equivariant message passing for the prediction of tensorial properties and molecular spectra* 2021. <https://arxiv.org/abs/2102.03150>.
74. Gasteiger, J., Groß, J. & Günnemann, S. *Directional Message Passing for Molecular Graphs* 2020. <https://arxiv.org/abs/2003.03123>.
75. Thölke, P. & De Fabritiis, G. TorchMD-NET: Equivariant Transformers for Neural Network based Molecular Potentials. *arXiv preprint arXiv:2202.02541* (2022).
76. Jing, B., Eismann, S., Suriana, P., Townshend, R. J. L. & Dror, R. *Learning from Protein Structure with Geometric Vector Perceptrons* in *International Conference on Learning Representations* (2021). <https://openreview.net/forum?id=1YLJDvSx6J4>.
77. Villar, S., Hogg, D. W., Storey-Fisher, K., Yao, W. & Blum-Smith, B. *Scalars are universal: Equivariant machine learning, structured like classical physics* in *Advances in Neural Information Processing Systems* (eds Beygelzimer, A., Dauphin, Y., Liang, P. & Vaughan, J. W.) (2021). <https://openreview.net/forum?id=ba27-RzNaIv>.
78. Finzi, M., Stanton, S., Izmailov, P. & Wilson, A. G. *Generalizing Convolutional Neural Networks for Equivariance to Lie Groups on Arbitrary Continuous Data* 2020. <https://arxiv.org/abs/2002.12880>.

79. Hutchinson, M., Lan, C. L., Zaidi, S., Dupont, E., Teh, Y. W. & Kim, H. *LieTransformer: Equivariant self-attention for Lie Groups* 2020. <https://arxiv.org/abs/2012.10885>.
80. Gasteiger, J., Becker, F. & Günemann, S. *GemNet: Universal Directional Graph Neural Networks for Molecules* 2021. <https://arxiv.org/abs/2106.08903>.
81. Liu, Y., Wang, L., Liu, M., Zhang, X., Oztekin, B. & Ji, S. *Spherical Message Passing for 3D Graph Networks* 2021. <https://arxiv.org/abs/2102.05013>.
82. Köhler, J., Klein, L. & Noé, F. *Equivariant Flows: Exact Likelihood Generative Learning for Symmetric Densities* 2020. <https://arxiv.org/abs/2006.02425>.
83. Huang, W., Han, J., Rong, Y., Xu, T., Sun, F. & Huang, J. *Equivariant Graph Mechanics Networks with Constraints* in *International Conference on Learning Representations* (2022). <https://openreview.net/forum?id=SHbhHHfePhP>.
84. Satorras, V. G., Hoogeboom, E. & Welling, M. *E(n) Equivariant Graph Neural Networks* 2021. <https://arxiv.org/abs/2102.09844>.
85. Mater, A. C. & Coote, M. L. Deep learning in chemistry. *Journal of chemical information and modeling* **59**, 2545–2559 (2019).
86. Wieder, O., Kohlbacher, S., Kuenemann, M., Garon, A., Ducrot, P., Seidel, T. & Langer, T. A compact review of molecular property prediction with graph neural networks. *Drug Discovery Today: Technologies* **37**, 1–12 (2020).
87. Xiong, J., Xiong, Z., Chen, K., Jiang, H. & Zheng, M. Graph neural networks for automated de novo drug design. *Drug Discovery Today* **26**, 1382–1393 (2021).
88. Coley, C. W., Barzilay, R., Green, W. H., Jaakkola, T. S. & Jensen, K. F. Convolutional embedding of attributed molecular graphs for physical property prediction. *Journal of chemical information and modeling* **57**, 1757–1772 (2017).
89. Deng, D., Chen, X., Zhang, R., Lei, Z., Wang, X. & Zhou, F. XGraph-Boost: extracting graph neural network-based features for a better prediction of molecular properties. *Journal of chemical information and modeling* **61**, 2697–2705 (2021).
90. Aldeghi, M., Graff, D. E., Frey, N., Morrone, J. A., Pyzer-Knapp, E. O., Jordan, K. E. & Coley, C. W. Roughness of molecular property landscapes and its impact on modellability. *arXiv preprint arXiv:2207.09250* (2022).
91. Cao, Z., Liu, V. & Barati Farimani, A. Water desalination with two-dimensional metal–organic framework membranes. *Nano Letters* **19**, 8638–8643 (2019).
92. Schwaller, P., Petraglia, R., Zullo, V., Nair, V. H., Haeuselmann, R. A., Pisoni, R., Bekas, C., Iuliano, A. & Laino, T. Predicting retrosynthetic pathways using transformer-based models and a hyper-graph exploration strategy. *Chemical science* **11**, 3316–3325 (2020).

93. Wu, Z., Ramsundar, B., Feinberg, E. N., Gomes, J., Geniesse, C., Pappu, A. S., Leswing, K. & Pande, V. MoleculeNet: a benchmark for molecular machine learning. *Chemical science* **9**, 513–530 (2018).
94. Dwivedi, V. P., Joshi, C. K., Laurent, T., Bengio, Y. & Bresson, X. Benchmarking graph neural networks. *arXiv preprint arXiv:2003.00982* (2020).
95. Irwin, J. J. & Shoichet, B. K. ZINC- a free database of commercially available compounds for virtual screening. *Journal of chemical information and modeling* **45**, 177–182 (2005).
96. Chen, G., Chen, P., Hsieh, C.-Y., Lee, C.-K., Liao, B., Liao, R., Liu, W., Qiu, J., Sun, Q., Tang, J., *et al.* Alchemy: A quantum chemistry dataset for benchmarking ai models. *arXiv preprint arXiv:1906.09427* (2019).
97. Smith, J. S., Isayev, O. & Roitberg, A. E. ANI-1, A data set of 20 million calculated off-equilibrium conformations for organic molecules. *Scientific data* **4**, 1–8 (2017).
98. Sanchez-Lengeling, B., Wei, J. N., Lee, B. K., Gerkin, R. C., Aspuru-Guzik, A. & Wiltschko, A. B. Machine learning for scent: Learning generalizable perceptual representations of small molecules. *arXiv preprint arXiv:1910.10685* (2019).
99. Lei, Z., Dai, C. & Chen, B. Gas solubility in ionic liquids. *Chemical reviews* **114**, 1289–1326 (2014).
100. Wang, Y., Wang, J., Cao, Z. & Barati Farimani, A. Molecular contrastive learning of representations via graph neural networks. *Nature Machine Intelligence*, 1–9 (2022).
101. Debnath, A. K., Lopez de Compadre, R. L., Debnath, G., Shusterman, A. J. & Hansch, C. Structure-activity relationship of mutagenic aromatic and heteroaromatic nitro compounds. correlation with molecular orbital energies and hydrophobicity. *Journal of medicinal chemistry* **34**, 786–797 (1991).
102. Kuhn, M., Letunic, I., Jensen, L. J. & Bork, P. The SIDER database of drugs and side effects. *Nucleic acids research* **44**, D1075–D1079 (2016).
103. Gayvert, K. M., Madhukar, N. S. & Elemento, O. A data-driven approach to predicting successes and failures of clinical trials. *Cell chemical biology* **23**, 1294–1301 (2016).
104. Martins, I. F., Teixeira, A. L., Pinheiro, L. & Falcao, A. O. A Bayesian approach to in silico blood-brain barrier penetration modeling. *Journal of chemical information and modeling* **52**, 1686–1697 (2012).
105. Wale, N., Watson, I. A. & Karypis, G. Comparison of descriptor spaces for chemical compound retrieval and classification. *Knowledge and Information Systems* **14**, 347–375 (2008).
106. *Tox21 Data Challenge 2014* <https://tripod.nih.gov/tox21/challenge/>.
107. Richard, A. M., Judson, R. S., Houck, K. A., Grulke, C. M., Volarath, P., Thillainadarajah, I., Yang, C., Rathman, J., Martin, M. T., Wambaugh, J. F., *et al.* ToxCast chemical landscape: paving the road to 21st century toxicology. *Chemical research in toxicology* **29**, 1225–1251 (2016).

108. Subramanian, G., Ramsundar, B., Pande, V. & Denny, R. A. Computational modeling of  $\beta$ -secretase 1 (BACE-1) inhibitors using ligand based approaches. *Journal of chemical information and modeling* **56**, 1936–1949 (2016).
109. Cortés-Ciriano, I. & Bender, A. KekuleScope: prediction of cancer cell line sensitivity and compound potency using convolutional neural networks trained on compound images. *Journal of Cheminformatics* **11**, 1–16 (2019).
110. Wang, R., Fang, X., Lu, Y. & Wang, S. The PDBbind database: Collection of binding affinities for protein- ligand complexes with known three-dimensional structures. *Journal of medicinal chemistry* **47**, 2977–2980 (2004).
111. Su, M., Yang, Q., Du, Y., Feng, G., Liu, Z., Li, Y. & Wang, R. Comparative assessment of scoring functions: the CASF-2016 update. *Journal of chemical information and modeling* **59**, 895–913 (2018).
112. AIDS antiviral screen data <https://wiki.nci.nih.gov/display/NCIDTPdata/AIDS+Antiviral+Screen+Data>.
113. Rohrer, S. G. & Baumann, K. Maximum unbiased validation (MUV) data sets for virtual screening based on PubChem bioactivity data. *Journal of chemical information and modeling* **49**, 169–184 (2009).
114. Wang, Y., Xiao, J., Suzek, T. O., Zhang, J., Wang, J., Zhou, Z., Han, L., Karapetyan, K., Dracheva, S., Shoemaker, B. A., *et al.* PubChem's BioAssay database. *Nucleic acids research* **40**, D400–D412 (2012).
115. Mobley, D. L. & Guthrie, J. P. FreeSolv: a database of experimental and calculated hydration free energies, with input files. *Journal of computer-aided molecular design* **28**, 711–720 (2014).
116. Delaney, J. S. ESOL: estimating aqueous solubility directly from molecular structure. *Journal of chemical information and computer sciences* **44**, 1000–1005 (2004).
117. Mendez, D., Gaulton, A., Bento, A. P., Chambers, J., De Veij, M., Félix, E., Magariños, M. P., Mosquera, J. F., Mutowo, P., Nowotka, M., *et al.* ChEMBL: towards direct deposition of bioassay data. *Nucleic acids research* **47**, D930–D940 (2019).
118. Sorkun, M. C., Khetan, A. & Er, S. AqSolDB, a curated reference set of aqueous solubility and 2D descriptors for a diverse set of compounds. *Scientific data* **6**, 1–8 (2019).
119. Rupp, M., Tkatchenko, A., Müller, K.-R. & Von Lilienfeld, O. A. Fast and accurate modeling of molecular atomization energies with machine learning. *Physical review letters* **108**, 058301 (2012).
120. Montavon, G., Rupp, M., Gobre, V., Vazquez-Mayagoitia, A., Hansen, K., Tkatchenko, A., Müller, K.-R. & von Lilienfeld, O. A. Machine learning of molecular electronic properties in chemical compound space. *New Journal of Physics* **15**, 095003 (2013).
121. Ruddigkeit, L., Van Deursen, R., Blum, L. C. & Reymond, J.-L. Enumeration of 166 billion organic small molecules in the chemical universe

database GDB-17. *Journal of chemical information and modeling* **52**, 2864–2875 (2012).

- 122. Ramakrishnan, R., Dral, P. O., Rupp, M. & von Lilienfeld, O. A. Quantum chemistry structures and properties of 134 kilo molecules. *Scientific Data* **1** (2014).
- 123. Hu, W., Fey, M., Zitnik, M., Dong, Y., Ren, H., Liu, B., Catasta, M. & Leskovec, J. Open graph benchmark: Datasets for machine learning on graphs. *Advances in neural information processing systems* **33**, 22118–22133 (2020).
- 124. Henaff, M., Bruna, J. & LeCun, Y. Deep convolutional networks on graph-structured data. *arXiv preprint arXiv:1506.05163* (2015).
- 125. Li, R., Wang, S., Zhu, F. & Huang, J. Adaptive graph convolutional neural networks in *Proceedings of the AAAI conference on artificial intelligence* **32** (2018).
- 126. Liao, R., Zhao, Z., Urtasun, R. & Zemel, R. S. Lanczosnet: Multi-scale deep graph convolutional networks. *arXiv preprint arXiv:1901.01484* (2019).
- 127. Ma, Y., Wang, S., Aggarwal, C. C. & Tang, J. Graph convolutional networks with eigenpooling in *Proceedings of the 25th ACM SIGKDD international conference on knowledge discovery & data mining* (2019), 723–731.
- 128. Xu, Y., Pei, J. & Lai, L. Deep learning based regression and multiclass models for acute oral toxicity prediction with automatic chemical feature extraction. *Journal of chemical information and modeling* **57**, 2672–2685 (2017).
- 129. Li, J., Cai, D. & He, X. Learning graph-level representation for drug discovery. *arXiv preprint arXiv:1709.03741* (2017).
- 130. Wang, X., Li, Z., Jiang, M., Wang, S., Zhang, S. & Wei, Z. Molecule property prediction based on spatial graph embedding. *Journal of chemical information and modeling* **59**, 3817–3828 (2019).
- 131. Cho, H. & Choi, I. S. Enhanced Deep-Learning Prediction of Molecular Properties via Augmentation of Bond Topology. *ChemMedChem* **14**, 1604–1609 (2019).
- 132. Feinberg, E. N., Joshi, E., Pande, V. S. & Cheng, A. C. Improvement in ADMET prediction with multitask deep featurization. *Journal of medicinal chemistry* **63**, 8835–8848 (2020).
- 133. Altae-Tran, H., Ramsundar, B., Pappu, A. S. & Pande, V. Low data drug discovery with one-shot learning. *ACS central science* **3**, 283–293 (2017).
- 134. Ryu, S., Lim, J., Hong, S. H. & Kim, W. Y. Deeply learning molecular structure-property relationships using attention-and gate-augmented graph convolutional network. *arXiv preprint arXiv:1805.10988* (2018).
- 135. Shindo, H. & Matsumoto, Y. Gated graph recursive neural networks for molecular property prediction. *arXiv preprint arXiv:1909.00259* (2019).
- 136. Withnall, M., Lindelöf, E., Engkvist, O. & Chen, H. Building attention and edge message passing neural networks for bioactivity and physical-chemical property prediction. *Journal of cheminformatics* **12**, 1–18 (2020).

137. Tang, B., Kramer, S. T., Fang, M., Qiu, Y., Wu, Z. & Xu, D. A self-attention based message passing neural network for predicting molecular lipophilicity and aqueous solubility. *Journal of cheminformatics* **12**, 1–9 (2020).
138. Ma, H., Bian, Y., Rong, Y., Huang, W., Xu, T., Xie, W., Ye, G. & Huang, J. Multi-view graph neural networks for molecular property prediction. *arXiv preprint arXiv:2005.13607* (2020).
139. Smith, J. S., Isayev, O. & Roitberg, A. E. ANI-1: an extensible neural network potential with DFT accuracy at force field computational cost. *Chemical science* **8**, 3192–3203 (2017).
140. Butler, K. T., Davies, D. W., Cartwright, H., Isayev, O. & Walsh, A. Machine learning for molecular and materials science. *Nature* **559**, 547–555 (2018).
141. Zhang, L., Han, J., Wang, H., Car, R. & Weinan, E. Deep potential molecular dynamics: a scalable model with the accuracy of quantum mechanics. *Physical review letters* **120**, 143001 (2018).
142. Lubbers, N., Smith, J. S. & Barros, K. Hierarchical modeling of molecular energies using a deep neural network. *The Journal of chemical physics* **148**, 241715 (2018).
143. Lu, C., Liu, Q., Wang, C., Huang, Z., Lin, P. & He, L. *Molecular property prediction: A multilevel quantum interactions modeling perspective* in *Proceedings of the AAAI Conference on Artificial Intelligence* **33** (2019), 1052–1060.
144. Anderson, B., Hy, T. S. & Kondor, R. Cormorant: Covariant molecular neural networks. *Advances in neural information processing systems* **32** (2019).
145. Liu, Y., Wang, L., Liu, M., Zhang, X., Oztekin, B. & Ji, S. Spherical message passing for 3d graph networks. *arXiv preprint arXiv:2102.05013* (2021).
146. Qiao, Z., Welborn, M., Anandkumar, A., Manby, F. R. & Miller III, T. F. OrbNet: Deep learning for quantum chemistry using symmetry-adapted atomic-orbital features. *The Journal of chemical physics* **153**, 124111 (2020).
147. Karamad, M., Magar, R., Shi, Y., Siahrostami, S., Gates, I. D. & Farimani, A. B. Orbital graph convolutional neural network for material property prediction. *Physical Review Materials* **4**, 093801 (2020).
148. Qiao, Z., Christensen, A. S., Welborn, M., Manby, F. R., Anandkumar, A. & Miller III, T. F. Informing geometric deep learning with electronic interactions to accelerate quantum chemistry. *Proceedings of the National Academy of Sciences* **119**, e2205221119 (2022).
149. Boiko, D., Reschützegger, T., Sanchez-Lengeling, B., Blau, S. & Gomes, G. Stereoelectronics-Aware Molecular Representation Learning (2022).
150. Satorras, V. G., Hoogeboom, E. & Welling, M. *E(n) equivariant graph neural networks* in *International conference on machine learning* (2021), 9323–9332.

151. Hutchinson, M. J., Le Lan, C., Zaidi, S., Dupont, E., Teh, Y. W. & Kim, H. *Lietransformer: Equivariant self-attention for lie groups* in *International Conference on Machine Learning* (2021), 4533–4543.
152. Miller, B. K., Geiger, M., Smidt, T. E. & Noé, F. Relevance of rotationally equivariant convolutions for predicting molecular properties. *arXiv preprint arXiv:2008.08461* (2020).
153. Gasteiger, J., Becker, F. & Günnemann, S. Gemnet: Universal directional graph neural networks for molecules. *Advances in Neural Information Processing Systems* **34**, 6790–6802 (2021).
154. Schütt, K., Unke, O. & Gastegger, M. *Equivariant message passing for the prediction of tensorial properties and molecular spectra* in *International Conference on Machine Learning* (2021), 9377–9388.
155. Chmiela, S., Tkatchenko, A., Sauceda, H. E., Poltavsky, I., Schütt, K. T. & Müller, K.-R. Machine learning of accurate energy-conserving molecular force fields. *Science advances* **3**, e1603015 (2017).
156. Hermann, J., Schätzle, Z. & Noé, F. Deep-neural-network solution of the electronic Schrödinger equation. *Nature Chemistry* **12**, 891–897 (2020).
157. Gao, N. & Günnemann, S. Ab-initio potential energy surfaces by pairing GNNs with neural wave functions. *arXiv preprint arXiv:2110.05064* (2021).
158. Stepniewska-Dziubinska, M. M., Zielenkiewicz, P. & Siedlecki, P. Development and evaluation of a deep learning model for protein–ligand binding affinity prediction. *Bioinformatics* **34**, 3666–3674 (2018).
159. McNutt, A. T., Francoeur, P., Aggarwal, R., Masuda, T., Meli, R., Ragoza, M., Sunseri, J. & Koes, D. R. GNINA 1.0: molecular docking with deep learning. *Journal of cheminformatics* **13**, 1–20 (2021).
160. Yang, L., Yang, G., Chen, X., Yang, Q., Yao, X., Bing, Z., Niu, Y., Huang, L. & Yang, L. Deep scoring neural network replacing the scoring function components to improve the performance of structure-based molecular docking. *ACS Chemical Neuroscience* **12**, 2133–2142 (2021).
161. Bao, J., He, X. & Zhang, J. Z. DeepBSP—a machine learning method for accurate prediction of protein–ligand docking structures. *Journal of Chemical Information and Modeling* **61**, 2231–2240 (2021).
162. Yadav, P., Mollaei, P., Cao, Z., Wang, Y. & Farimani, A. B. Prediction of GPCR activity using Machine Learning. *Computational and Structural Biotechnology Journal* (2022).
163. Wang, R., Fang, X., Lu, Y., Yang, C.-Y. & Wang, S. The PDBbind database: methodologies and updates. *Journal of medicinal chemistry* **48**, 4111–4119 (2005).
164. Liu, Z., Su, M., Han, L., Liu, J., Yang, Q., Li, Y. & Wang, R. Forging the basis for developing protein–ligand interaction scoring functions. *Accounts of chemical research* **50**, 302–309 (2017).
165. Mysinger, M. M., Carchia, M., Irwin, J. J. & Shoichet, B. K. Directory of useful decoys, enhanced (DUD-E): better ligands and decoys for better benchmarking. *Journal of medicinal chemistry* **55**, 6582–6594 (2012).

166. Liu, T., Lin, Y., Wen, X., Jorissen, R. N. & Gilson, M. K. BindingDB: a web-accessible database of experimentally determined protein–ligand binding affinities. *Nucleic acids research* **35**, D198–D201 (2007).
167. Gilson, M. K., Liu, T., Baitaluk, M., Nicola, G., Hwang, L. & Chong, J. BindingDB in 2015: a public database for medicinal chemistry, computational chemistry and systems pharmacology. *Nucleic acids research* **44**, D1045–D1053 (2016).
168. Wishart, D. S., Knox, C., Guo, A. C., Shrivastava, S., Hassanali, M., Stothard, P., Chang, Z. & Woolsey, J. DrugBank: a comprehensive resource for in silico drug discovery and exploration. *Nucleic acids research* **34**, D668–D672 (2006).
169. Wishart, D. S., Knox, C., Guo, A. C., Cheng, D., Shrivastava, S., Tzur, D., Gautam, B. & Hassanali, M. DrugBank: a knowledgebase for drugs, drug actions and drug targets. *Nucleic acids research* **36**, D901–D906 (2008).
170. Gao, K. Y., Fokoue, A., Luo, H., Iyengar, A., Dey, S., Zhang, P., *et al.* *Interpretable Drug Target Prediction Using Deep Neural Representation*. in *IJCAI 2018* (2018), 3371–3377.
171. Zheng, S., Li, Y., Chen, S., Xu, J. & Yang, Y. Predicting drug–protein interaction using quasi-visual question answering system. *Nature Machine Intelligence* **2**, 134–140 (2020).
172. Lim, S., Lu, Y., Cho, C. Y., Sung, I., Kim, J., Kim, Y., Park, S. & Kim, S. A review on compound–protein interaction prediction methods: data, format, representation and model. *Computational and Structural Biotechnology Journal* **19**, 1541–1556 (2021).
173. Karimi, M., Wu, D., Wang, Z. & Shen, Y. DeepAffinity: interpretable deep learning of compound–protein affinity through unified recurrent and convolutional neural networks. *Bioinformatics* **35**, 3329–3338 (2019).
174. Li, H., Lu, G., Sze, K.-H., Su, X., Chan, W.-Y. & Leung, K.-S. Machine-learning scoring functions trained on complexes dissimilar to the test set already outperform classical counterparts on a blind benchmark. *Briefings in bioinformatics* **22**, bbab225 (2021).
175. Li, S., Zhou, J., Xu, T., Huang, L., Wang, F., Xiong, H., Huang, W., Dou, D. & Xiong, H. *Structure-aware interactive graph neural networks for the prediction of protein–ligand binding affinity* in *Proceedings of the 27th ACM SIGKDD Conference on Knowledge Discovery & Data Mining* (2021), 975–985.
176. Feinberg, E. N., Sur, D., Wu, Z., Husic, B. E., Mai, H., Li, Y., Sun, S., Yang, J., Ramsundar, B. & Pande, V. S. PotentialNet for molecular property prediction. *ACS central science* **4**, 1520–1530 (2018).
177. Gomes, J., Ramsundar, B., Feinberg, E. N. & Pande, V. S. Atomic convolutional networks for predicting protein–ligand binding affinity. *arXiv preprint arXiv:1703.10603* (2017).
178. Lim, J., Ryu, S., Park, K., Choe, Y. J., Ham, J. & Kim, W. Y. Predicting drug–target interaction using a novel graph neural network with 3D

structure-embedded graph representation. *Journal of chemical information and modeling* **59**, 3981–3988 (2019).

- 179. Jiang, D., Hsieh, C.-Y., Wu, Z., Kang, Y., Wang, J., Wang, E., Liao, B., Shen, C., Xu, L., Wu, J., *et al.* Interactiongraphnet: A novel and efficient deep graph representation learning framework for accurate protein–ligand interaction predictions. *Journal of medicinal chemistry* **64**, 18209–18232 (2021).
- 180. Morrone, J. A., Weber, J. K., Huynh, T., Luo, H. & Cornell, W. D. Combining docking pose rank and structure with deep learning improves protein–ligand binding mode prediction over a baseline docking approach. *Journal of chemical information and modeling* **60**, 4170–4179 (2020).
- 181. Son, J. & Kim, D. Development of a graph convolutional neural network model for efficient prediction of protein-ligand binding affinities. *PLoS one* **16**, e0249404 (2021).
- 182. Knutson, C., Bontha, M., Bilbrey, J. A. & Kumar, N. Decoding the protein–ligand interactions using parallel graph neural networks. *Scientific reports* **12**, 1–14 (2022).
- 183. Torng, W. & Altman, R. B. Graph convolutional neural networks for predicting drug-target interactions. *Journal of chemical information and modeling* **59**, 4131–4149 (2019).
- 184. Nguyen, T., Le, H., Quinn, T. P., Nguyen, T., Le, T. D. & Venkatesh, S. GraphDTA: Predicting drug–target binding affinity with graph neural networks. *Bioinformatics* **37**, 1140–1147 (2021).
- 185. Moesser, M. A., Klein, D., Boyles, F., Deane, C. M., Baxter, A. & Morris, G. M. Protein-Ligand Interaction Graphs: Learning from Ligand-Shaped 3D Interaction Graphs to Improve Binding Affinity Prediction. *bioRxiv* (2022).
- 186. Wang, J., Li, X. & Zhang, H. GNN-PT: enhanced prediction of compound–protein interactions by integrating protein transformer. *arXiv preprint arXiv:2009.00805* (2020).
- 187. Wang, P., Zheng, S., Jiang, Y., Li, C., Liu, J., Wen, C., Patronov, A., Qian, D., Chen, H. & Yang, Y. Structure-aware multimodal deep learning for drug–protein interaction prediction. *Journal of chemical information and modeling* **62**, 1308–1317 (2022).
- 188. Yang, Z., Zhong, W., Zhao, L. & Chen, C. Y.-C. MGraphDTA: deep multiscale graph neural network for explainable drug–target binding affinity prediction. *Chemical science* **13**, 816–833 (2022).
- 189. Lengauer, T. & Rarey, M. Computational methods for biomolecular docking. *Current opinion in structural biology* **6**, 402–406 (1996).
- 190. Kitchen, D. B., Decornez, H., Furr, J. R. & Bajorath, J. Docking and scoring in virtual screening for drug discovery: methods and applications. *Nature reviews Drug discovery* **3**, 935–949 (2004).
- 191. Ciemny, M., Kurcinski, M., Kamel, K., Kolinski, A., Alam, N., Schueler-Furman, O. & Kmiecik, S. Protein-peptide docking: opportunities and challenges. *Drug discovery today* **23**, 1530–1537 (2018).

192. Erickson, J. A., Jalaie, M., Robertson, D. H., Lewis, R. A. & Vieth, M. Lessons in molecular recognition: the effects of ligand and protein flexibility on molecular docking accuracy. *Journal of medicinal chemistry* **47**, 45–55 (2004).
193. Wang, Z., Sun, H., Yao, X., Li, D., Xu, L., Li, Y., Tian, S. & Hou, T. Comprehensive evaluation of ten docking programs on a diverse set of protein–ligand complexes: the prediction accuracy of sampling power and scoring power. *Physical Chemistry Chemical Physics* **18**, 12964–12975 (2016).
194. Ganea, O.-E., Huang, X., Bunne, C., Bian, Y., Barzilay, R., Jaakkola, T. & Krause, A. Independent se (3)-equivariant models for end-to-end rigid protein docking. *arXiv preprint arXiv:2111.07786* (2021).
195. Garcíá-Ortegón, M., Simm, G. N., Tripp, A. J., Hernández-Lobato, J. M., Bender, A. & Bacallado, S. DOCKSTRING: easy molecular docking yields better benchmarks for ligand design. *Journal of Chemical Information and Modeling* (2021).
196. Jin, W., Barzilay, R. & Jaakkola, T. Antibody-Antigen Docking and Design via Hierarchical Equivariant Refinement. *arXiv preprint arXiv:2207.06616* (2022).
197. Shen, C., Zhang, X., Deng, Y., Gao, J., Wang, D., Xu, L., Pan, P., Hou, T. & Kang, Y. Boosting Protein–Ligand Binding Pose Prediction and Virtual Screening Based on Residue–Atom Distance Likelihood Potential and Graph Transformer. *Journal of Medicinal Chemistry* (2022).
198. Jiang, H., Wang, J., Cong, W., Huang, Y., Ramezani, M., Sarma, A., Dokholyan, N. V., Mahdavi, M. & Kandemir, M. T. Predicting Protein–Ligand Docking Structure with Graph Neural Network. *Journal of Chemical Information and Modeling* **62**, 2923–2932 (2022).
199. Méndez-Lucio, O., Ahmad, M., del Rio-Chanona, E. A. & Wegner, J. K. A geometric deep learning approach to predict binding conformations of bioactive molecules. *Nature Machine Intelligence* **3**, 1033–1039 (2021).
200. Klebe, G. & Mietzner, T. A fast and efficient method to generate biologically relevant conformations. *Journal of Computer-Aided Molecular Design* **8**, 583–606 (1994).
201. Li, L. & Cai, M. Drug target prediction by multi-view low rank embedding. *IEEE/ACM transactions on computational biology and bioinformatics* **16**, 1712–1721 (2017).
202. Dai, B. & Bailey-Kellogg, C. Protein interaction interface region prediction by geometric deep learning. *Bioinformatics* **37**, 2580–2588 (2021).
203. Sverrisson, F., Feydy, J., Southern, J., Bronstein, M. M. & Correia, B. *Physics-informed deep neural network for rigid-body protein docking in ICLR2022 Machine Learning for Drug Discovery* (2022).
204. Zong, N., Li, N., Wen, A., Ngo, V., Yu, Y., Huang, M., Chowdhury, S., Jiang, C., Fu, S., Weinshilboum, R., *et al.* BETA: a comprehensive benchmark for computational drug–target prediction. *Briefings in Bioinformatics* (2022).

205. Stärk, H., Ganea, O., Pattanaik, L., Barzilay, R. & Jaakkola, T. *Equibind: Geometric deep learning for drug binding structure prediction* in *International Conference on Machine Learning* (2022), 20503–20521.
206. Lu, W., Wu, Q., Zhang, J., Rao, J., Li, C. & Zheng, S. TANKBind: Trigonometry-Aware Neural NetworKs for Drug-Protein Binding Structure Prediction. *bioRxiv* (2022).
207. Hollingsworth, S. A. & Dror, R. O. Molecular Dynamics Simulation for All. *Neuron* **99**, 1129–1143. ISSN: 0896-6273. <https://www.sciencedirect.com/science/article/pii/S0896627318306846> (2018).
208. Karplus, M. & McCammon, J. A. Molecular dynamics simulations of biomolecules. *Nature Structural Biology* **9**, 646–652. ISSN: 1545-9985. <https://doi.org/10.1038/nsb0902-646> (2002).
209. De Vivo, M., Masetti, M., Bottegoni, G. & Cavalli, A. Role of Molecular Dynamics and Related Methods in Drug Discovery. *Journal of Medicinal Chemistry* **59**. PMID: 26807648, 4035–4061. eprint: <https://doi.org/10.1021/acs.jmedchem.5b01684>. <https://doi.org/10.1021/acs.jmedchem.5b01684> (2016).
210. Becke, A. D. Perspective: Fifty years of density-functional theory in chemical physics. *The Journal of Chemical Physics* **140**, 18A301. eprint: <https://doi.org/10.1063/1.4869598>. <https://doi.org/10.1063/1.4869598> (2014).
211. Harrison, J. A., Schall, J. D., Maskey, S., Mikulski, P. T., Knippenberg, M. T. & Morrow, B. H. Review of force fields and intermolecular potentials used in atomistic computational materials research. *Applied Physics Reviews* **5**, 031104. eprint: <https://doi.org/10.1063/1.5020808>. <https://doi.org/10.1063/1.5020808> (2018).
212. Bartók, A. P., De, S., Poelking, C., Bernstein, N., Kermode, J. R., Csányi, G. & Ceriotti, M. Machine learning unifies the modeling of materials and molecules. *Science Advances* **3**. eprint: <https://advances.sciencemag.org/content/3/12/e1701816.full.pdf>. <https://advances.sciencemag.org/content/3/12/e1701816> (2017).
213. Deringer, V. L., Caro, M. A. & Csányi, G. Machine Learning Interatomic Potentials as Emerging Tools for Materials Science. *Advanced Materials* **31**, 1902765. eprint: <https://onlinelibrary.wiley.com/doi/pdf/10.1002/adma.201902765>. <https://onlinelibrary.wiley.com/doi/abs/10.1002/adma.201902765> (2019).
214. Gkeka, P., Stoltz, G., Barati Farimani, A., Belkacemi, Z., Ceriotti, M., Chodera, J. D., Danner, A. R., Ferguson, A. L., Maillet, J.-B., Minoux, H., Peter, C., Pietrucci, F., Silveira, A., Tkatchenko, A., Trstanova, Z., Wiewiora, R. & Lelièvre, T. Machine Learning Force Fields and Coarse-Grained Variables in Molecular Dynamics: Application to Materials and Biological Systems. *Journal of Chemical Theory and Computation* **16**. PMID: 32559068, 4757–4775. eprint: <https://doi.org/10.1021/acs.jctc.0c00355>. <https://doi.org/10.1021/acs.jctc.0c00355> (2020).

215. Noé, F., Tkatchenko, A., Müller, K.-R. & Clementi, C. Machine Learning for Molecular Simulation. *Annual Review of Physical Chemistry* **71**. PMID: 32092281, 361–390. eprint: <https://doi.org/10.1146/annurev-physchem-042018-052331> (2020).
216. Chen, C., Ye, W., Zuo, Y., Zheng, C. & Ong, S. P. Graph Networks as a Universal Machine Learning Framework for Molecules and Crystals. *Chemistry of Materials* **31**, 3564–3572. eprint: <https://doi.org/10.1021/acs.chemmater.9b01294>. <https://doi.org/10.1021/acs.chemmater.9b01294> (2019).
217. Li, Y., Li, H., Pickard, F. C., Narayanan, B., Sen, F. G., Chan, M. K. Y., Sankaranarayanan, S. K. R. S., Brooks, B. R. & Roux, B. Machine Learning Force Field Parameters from Ab Initio Data. *Journal of Chemical Theory and Computation* **13**. PMID: 28800233, 4492–4503. eprint: <https://doi.org/10.1021/acs.jctc.7b00521>. <https://doi.org/10.1021/acs.jctc.7b00521> (2017).
218. Christensen, A. S., Bratholm, L. A., Faber, F. A. & Anatole von Lilienfeld, O. FCHL revisited: Faster and more accurate quantum machine learning. *The Journal of Chemical Physics* **152**, 044107. eprint: <https://doi.org/10.1063/1.5126701>. <https://doi.org/10.1063/1.5126701> (2020).
219. Zhang, L., Han, J., Wang, H., Car, R. & E, W. Deep Potential Molecular Dynamics: A Scalable Model with the Accuracy of Quantum Mechanics. *Phys. Rev. Lett.* **120**, 143001. <https://link.aps.org/doi/10.1103/PhysRevLett.120.143001> (14 2018).
220. Carbogno, C., Behler, J., Groß, A. & Reuter, K. Fingerprints for Spin-Selection Rules in the Interaction Dynamics of O<sub>2</sub> at Al(111). *Phys. Rev. Lett.* **101**, 096104. <https://link.aps.org/doi/10.1103/PhysRevLett.101.096104> (9 2008).
221. Behler, J. Atom-centered symmetry functions for constructing high-dimensional neural network potentials. *The Journal of Chemical Physics* **134**, 074106. eprint: <https://doi.org/10.1063/1.3553717>. <https://doi.org/10.1063/1.3553717> (2011).
222. Behler, J. & Parrinello, M. Generalized Neural-Network Representation of High-Dimensional Potential-Energy Surfaces. *Phys. Rev. Lett.* **98**, 146401. <https://link.aps.org/doi/10.1103/PhysRevLett.98.146401> (14 2007).
223. Behler, J. First Principles Neural Network Potentials for Reactive Simulations of Large Molecular and Condensed Systems. *Angewandte Chemie International Edition* **56**, 12828–12840. eprint: <https://onlinelibrary.wiley.com/doi/10.1002/anie.201703114>. <https://onlinelibrary.wiley.com/doi/abs/10.1002/anie.201703114> (2017).
224. Zubatyuk, R., Smith, J. S., Leszczynski, J. & Isayev, O. Accurate and transferable multitask prediction of chemical properties with an atoms-in-molecules neural network. *Science advances* **5**, eaav6490 (2019).

225. Behler, J. Perspective: Machine learning potentials for atomistic simulations. *The Journal of Chemical Physics* **145**, 170901. eprint: <https://doi.org/10.1063/1.4966192>. <https://doi.org/10.1063/1.4966192> (2016).
226. Rupp, M., Tkatchenko, A., Müller, K.-R. & von Lilienfeld, O. A. Fast and Accurate Modeling of Molecular Atomization Energies with Machine Learning. *Phys. Rev. Lett.* **108**, 058301 (5 2012).
227. Zhang, L., Han, J., Wang, H., Car, R. & E, W. Deep Potential Molecular Dynamics: A Scalable Model with the Accuracy of Quantum Mechanics. *Phys. Rev. Lett.* **120**, 143001. <https://link.aps.org/doi/10.1103/PhysRevLett.120.143001> (14 2018).
228. Hu, W., Shuaibi, M., Das, A., Goyal, S., Sriram, A., Leskovec, J., Parikh, D. & Zitnick, C. L. *ForceNet: A Graph Neural Network for Large-Scale Quantum Calculations* 2021. <https://arxiv.org/abs/2103.01436>.
229. Mailoa, J. P., Kornbluth, M., Batzner, S., Samsonidze, G., Lam, S. T., Vandermause, J., Abllitt, C., Molinari, N. & Kozinsky, B. A fast neural network approach for direct covariant forces prediction in complex multi-element extended systems. *Nature Machine Intelligence* **1**, 471–479. <https://doi.org/10.1038%2Fs42256-019-0098-0> (2019).
230. Park, C. W., Kornbluth, M., Vandermause, J., Wolverton, C., Kozinsky, B. & Mailoa, J. Accurate and scalable graph neural network force field and molecular dynamics with direct force architecture. *npj Computational Materials* **7** (2021).
231. Li, Z., Meidani, K., Yadav, P. & Barati Farimani, A. Graph neural networks accelerated molecular dynamics. *The Journal of Chemical Physics* **156**, 144103 (2022).
232. Wu, F., Zhang, Q., Jin, X., Jiang, Y. & Li, S. Z. *A Score-based Geometric Model for Molecular Dynamics Simulations* 2022. <https://arxiv.org/abs/2204.08672>.
233. Fu, X., Xie, T., Rebello, N. J., Olsen, B. D. & Jaakkola, T. *Simulate Time-integrated Coarse-grained Molecular Dynamics with Geometric Machine Learning* 2022. <https://arxiv.org/abs/2204.10348>.
234. Noé, F., Olsson, S., Köhler, J. & Wu, H. *Boltzmann Generators – Sampling Equilibrium States of Many-Body Systems with Deep Learning* 2018. <https://arxiv.org/abs/1812.01729>.
235. Mahmoud, A. H., Masters, M., Lee, S. J. & Lill, M. A. Accurate Sampling of Macromolecular Conformations Using Adaptive Deep Learning and Coarse-Grained Representation. *Journal of Chemical Information and Modeling* **62**. PMID: 35352898, 1602–1617. eprint: <https://doi.org/10.1021/acs.jcim.1c01438>. <https://doi.org/10.1021/acs.jcim.1c01438> (2022).
236. Elton, D. C., Boukouvalas, Z., Fuge, M. D. & Chung, P. W. Deep learning for molecular design—a review of the state of the art. *Molecular Systems Design & Engineering* **4**, 828–849 (2019).

237. DiMasi, J. A., Grabowski, H. G. & Hansen, R. W. Innovation in the pharmaceutical industry: new estimates of R&D costs. *Journal of health economics* **47**, 20–33 (2016).
238. Yang, X., Wang, Y., Byrne, R., Schneider, G. & Yang, S. Concepts of artificial intelligence for computer-assisted drug discovery. *Chemical reviews* **119**, 10520–10594 (2019).
239. Dimitrov, T., Kreisbeck, C., Becker, J. S., Aspuru-Guzik, A. & Saikin, S. K. Autonomous molecular design: then and now. *ACS applied materials & interfaces* **11**, 24825–24836 (2019).
240. Schneider, P., Walters, W. P., Plowright, A. T., Sieroka, N., Listgarten, J., Goodnow, R. A., Fisher, J., Jansen, J. M., Duca, J. S., Rush, T. S., *et al.* Rethinking drug design in the artificial intelligence era. *Nature Reviews Drug Discovery* **19**, 353–364 (2020).
241. Jiménez-Luna, J., Grisoni, F. & Schneider, G. Drug discovery with explainable artificial intelligence. *Nature Machine Intelligence* **2**, 573–584 (2020).
242. Xie, W., Wang, F., Li, Y., Lai, L. & Pei, J. Advances and Challenges in De Novo Drug Design Using Three-Dimensional Deep Generative Models. *Journal of Chemical Information and Modeling* (2022).
243. Sun, M., Zhao, S., Gilvary, C., Elemento, O., Zhou, J. & Wang, F. Graph convolutional networks for computational drug development and discovery. *Briefings in bioinformatics* **21**, 919–935 (2020).
244. Popova, M., Shvets, M., Oliva, J. & Isayev, O. MolecularRNN: Generating realistic molecular graphs with optimized properties. *arXiv preprint arXiv:1905.13372* (2019).
245. Bongini, P., Bianchini, M. & Scarselli, F. Molecular generative graph neural networks for drug discovery. *Neurocomputing* **450**, 242–252 (2021).
246. Kingma, D. P. & Welling, M. Auto-encoding variational bayes. *arXiv preprint arXiv:1312.6114* (2013).
247. Goodfellow, I., Pouget-Abadie, J., Mirza, M., Xu, B., Warde-Farley, D., Ozair, S., Courville, A. & Bengio, Y. Generative adversarial nets. *Advances in neural information processing systems* **27** (2014).
248. Rezende, D. & Mohamed, S. *Variational inference with normalizing flows* in *International conference on machine learning* (2015), 1530–1538.
249. Song, Y. & Ermon, S. Generative modeling by estimating gradients of the data distribution. *Advances in Neural Information Processing Systems* **32** (2019).
250. Ho, J., Jain, A. & Abbeel, P. Denoising diffusion probabilistic models. *Advances in Neural Information Processing Systems* **33**, 6840–6851 (2020).
251. Brown, N., Fiscato, M., Segler, M. H. & Vaucher, A. C. GuacaMol: benchmarking models for de novo molecular design. *Journal of chemical information and modeling* **59**, 1096–1108 (2019).
252. Polykovskiy, D., Zhebrak, A., Sanchez-Lengeling, B., Golovanov, S., Tatanov, O., Belyaev, S., Kurbanov, R., Artamonov, A., Aladinskiy, V., Veselov,

M., *et al.* Molecular sets (MOSES): a benchmarking platform for molecular generation models. *Frontiers in pharmacology* **11**, 565644 (2020).

- 253. Preuer, K., Renz, P., Unterthiner, T., Hochreiter, S. & Klambauer, G. Fréchet ChemNet distance: a metric for generative models for molecules in drug discovery. *Journal of chemical information and modeling* **58**, 1736–1741 (2018).
- 254. Heusel, M., Ramsauer, H., Unterthiner, T., Nessler, B. & Hochreiter, S. Gans trained by a two time-scale update rule converge to a local nash equilibrium. *Advances in neural information processing systems* **30** (2017).
- 255. Gómez-Bombarelli, R., Wei, J. N., Duvenaud, D., Hernández-Lobato, J. M., Sánchez-Lengeling, B., Sheberla, D., Aguilera-Iparraguirre, J., Hirzel, T. D., Adams, R. P. & Aspuru-Guzik, A. Automatic chemical design using a data-driven continuous representation of molecules. *ACS central science* **4**, 268–276 (2018).
- 256. Ertl, P. & Schuffenhauer, A. Estimation of synthetic accessibility score of drug-like molecules based on molecular complexity and fragment contributions. *Journal of cheminformatics* **1**, 1–11 (2009).
- 257. Bickerton, G. R., Paolini, G. V., Besnard, J., Muresan, S. & Hopkins, A. L. Quantifying the chemical beauty of drugs. *Nature chemistry* **4**, 90–98 (2012).
- 258. Gretton, A., Borgwardt, K. M., Rasch, M. J., Schölkopf, B. & Smola, A. A kernel two-sample test. *The Journal of Machine Learning Research* **13**, 723–773 (2012).
- 259. You, J., Ying, R., Ren, X., Hamilton, W. & Leskovec, J. *Graphrnn: Generating realistic graphs with deep auto-regressive models* in *International conference on machine learning* (2018), 5708–5717.
- 260. Friesner, R. A., Banks, J. L., Murphy, R. B., Halgren, T. A., Klicic, J. J., Mainz, D. T., Repasky, M. P., Knoll, E. H., Shelley, M., Perry, J. K., *et al.* Glide: a new approach for rapid, accurate docking and scoring. 1. Method and assessment of docking accuracy. *Journal of medicinal chemistry* **47**, 1739–1749 (2004).
- 261. Trott, O. & Olson, A. J. AutoDock Vina: improving the speed and accuracy of docking with a new scoring function, efficient optimization, and multithreading. *Journal of computational chemistry* **31**, 455–461 (2010).
- 262. Eastman, P., Swails, J., Chodera, J. D., McGibbon, R. T., Zhao, Y., Beauchamp, K. A., Wang, L.-P., Simmonett, A. C., Harrigan, M. P., Stern, C. D., *et al.* OpenMM 7: Rapid development of high performance algorithms for molecular dynamics. *PLoS computational biology* **13**, e1005659 (2017).
- 263. Hollingsworth, S. A. & Dror, R. O. Molecular dynamics simulation for all. *Neuron* **99**, 1129–1143 (2018).
- 264. Cournia, Z., Allen, B. K., Beuming, T., Pearlman, D. A., Radak, B. K. & Sherman, W. Rigorous free energy simulations in virtual screening. *Journal of Chemical Information and Modeling* **60**, 4153–4169 (2020).

265. Jeon, W. & Kim, D. Autonomous molecule generation using reinforcement learning and docking to develop potential novel inhibitors. *Scientific reports* **10**, 1–11 (2020).
266. Eckmann, P., Sun, K., Zhao, B., Feng, M., Gilson, M. K. & Yu, R. LIMO: Latent Inceptionism for Targeted Molecule Generation. *arXiv preprint arXiv:2206.09010* (2022).
267. Hoogeboom, E., Satorras, V. G., Vignac, C. & Welling, M. *Equivariant diffusion for molecule generation in 3d* in *International Conference on Machine Learning* (2022), 8867–8887.
268. Gao, W., Fu, T., Sun, J. & Coley, C. W. Sample Efficiency Matters: A Benchmark for Practical Molecular Optimization. *arXiv preprint arXiv:2206.12411* (2022).
269. Blum, L. C. & Reymond, J.-L. 970 million druglike small molecules for virtual screening in the chemical universe database GDB-13. *Journal of the American Chemical Society* **131**, 8732–8733 (2009).
270. Axelrod, S. & Gomez-Bombarelli, R. GEOM, energy-annotated molecular conformations for property prediction and molecular generation. *Scientific Data* **9**, 1–14 (2022).
271. Grover, A., Zweig, A. & Ermon, S. *Graphite: Iterative generative modeling of graphs* in *International conference on machine learning* (2019), 2434–2444.
272. Olivcrona, M., Blaschke, T., Engkvist, O. & Chen, H. Molecular de-novo design through deep reinforcement learning. *Journal of cheminformatics* **9**, 1–14 (2017).
273. Guimaraes, G. L., Sanchez-Lengeling, B., Outeiral, C., Farias, P. L. C. & Aspuru-Guzik, A. Objective-reinforced generative adversarial networks (ORGAN) for sequence generation models. *arXiv preprint arXiv:1705.10843* (2017).
274. Zhavoronkov, A., Ivanenkov, Y. A., Aliper, A., Veselov, M. S., Aladinskiy, V. A., Aladinskaya, A. V., Terentiev, V. A., Polykovskiy, D. A., Kuznetsov, M. D., Asadulaev, A., *et al.* Deep learning enables rapid identification of potent DDR1 kinase inhibitors. *Nature biotechnology* **37**, 1038–1040 (2019).
275. Zhou, Z., Kearnes, S., Li, L., Zare, R. N. & Riley, P. Optimization of molecules via deep reinforcement learning. *Scientific reports* **9**, 1–10 (2019).
276. Wang, Y., Cao, Z. & Barati Farimani, A. Efficient water desalination with graphene nanopores obtained using artificial intelligence. *npj 2D Materials and Applications* **5**, 1–9 (2021).
277. Grebner, C., Matter, H., Plowright, A. T. & Hessler, G. Automated de novo design in medicinal chemistry: which types of chemistry does a generative neural network learn? *Journal of Medicinal Chemistry* **63**, 8809–8823 (2020).
278. You, J., Liu, B., Ying, Z., Pande, V. & Leskovec, J. Graph convolutional policy network for goal-directed molecular graph generation. *Advances in neural information processing systems* **31** (2018).

279. Jin, W., Barzilay, R. & Jaakkola, T. *Multi-objective molecule generation using interpretable substructures* in *International conference on machine learning* (2020), 4849–4859.
280. Li, Y., Zhang, L. & Liu, Z. Multi-objective de novo drug design with conditional graph generative model. *Journal of cheminformatics* **10**, 1–24 (2018).
281. Khemchandani, Y., O'Hagan, S., Samanta, S., Swainston, N., Roberts, T. J., Bollegala, D. & Kell, D. B. DeepGraphMolGen, a multi-objective, computational strategy for generating molecules with desirable properties: a graph convolution and reinforcement learning approach. *Journal of cheminformatics* **12**, 1–17 (2020).
282. Mercado, R., Rastemo, T., Lindelöf, E., Klambauer, G., Engkvist, O., Chen, H. & Bjerrum, E. J. Graph networks for molecular design. *Machine Learning: Science and Technology* **2**, 025023 (2021).
283. Podda, M., Bacciu, D. & Micheli, A. *A deep generative model for fragment-based molecule generation* in *International Conference on Artificial Intelligence and Statistics* (2020), 2240–2250.
284. Chen, Z., Min, M. R., Parthasarathy, S. & Ning, X. A deep generative model for molecule optimization via one fragment modification. *Nature Machine Intelligence* **3**, 1040–1049 (2021).
285. Lim, J., Hwang, S.-Y., Moon, S., Kim, S. & Kim, W. Y. Scaffold-based molecular design with a graph generative model. *Chemical science* **11**, 1153–1164 (2020).
286. Xie, Y., Shi, C., Zhou, H., Yang, Y., Zhang, W., Yu, Y. & Li, L. Mars: Markov molecular sampling for multi-objective drug discovery. *arXiv preprint arXiv:2103.10432* (2021).
287. Shi, C., Xu, M., Zhu, Z., Zhang, W., Zhang, M. & Tang, J. Graphaf: a flow-based autoregressive model for molecular graph generation. *arXiv preprint arXiv:2001.09382* (2020).
288. Luo, Y., Yan, K. & Ji, S. *Graphdf: A discrete flow model for molecular graph generation* in *International Conference on Machine Learning* (2021), 7192–7203.
289. Gebauer, N., Gastegger, M. & Schütt, K. Symmetry-adapted generation of 3d point sets for the targeted discovery of molecules. *Advances in neural information processing systems* **32** (2019).
290. Gebauer, N. W., Gastegger, M., Hessmann, S. S., Müller, K.-R. & Schütt, K. T. Inverse design of 3d molecular structures with conditional generative neural networks. *Nature communications* **13**, 1–11 (2022).
291. Simm, G., Pinsler, R. & Hernández-Lobato, J. M. *Reinforcement learning for molecular design guided by quantum mechanics* in *International Conference on Machine Learning* (2020), 8959–8969.
292. Flam-Shepherd, D., Zhigalin, A. & Aspuru-Guzik, A. Scalable Fragment-Based 3D Molecular Design with Reinforcement Learning. *arXiv preprint arXiv:2202.00658* (2022).

293. Luo, Y. & Ji, S. *An autoregressive flow model for 3d molecular geometry generation from scratch* in *International Conference on Learning Representations* (2021).
294. Luo, S., Guan, J., Ma, J. & Peng, J. A 3D generative model for structure-based drug design. *Advances in Neural Information Processing Systems* **34**, 6229–6239 (2021).
295. Liu, M., Luo, Y., Uchino, K., Maruhashi, K. & Ji, S. Generating 3D Molecules for Target Protein Binding. *arXiv preprint arXiv:2204.09410* (2022).
296. Powers, A., Yu, H., Suriana, P. & Dror, R. Fragment-Based Ligand Generation Guided by Geometric Deep Learning on Protein-Ligand Structure. *bioRxiv* (2022).
297. Imrie, F., Bradley, A. R., van der Schaar, M. & Deane, C. M. Deep generative models for 3D linker design. *Journal of chemical information and modeling* **60**, 1983–1995 (2020).
298. Blaschke, T., Olivecrona, M., Engkvist, O., Bajorath, J. & Chen, H. Application of generative autoencoder in de novo molecular design. *Molecular informatics* **37**, 1700123 (2018).
299. Kipf, T. N. & Welling, M. Variational graph auto-encoders. *arXiv preprint arXiv:1611.07308* (2016).
300. Kusner, M. J., Paige, B. & Hernández-Lobato, J. M. *Grammar variational autoencoder* in *International conference on machine learning* (2017), 1945–1954.
301. Vignac, C. & Frossard, P. *Top-N: Equivariant Set and Graph Generation without Exchangeability* in *International Conference on Learning Representations* (2022).
302. Simonovsky, M. & Komodakis, N. *Graphvae: Towards generation of small graphs using variational autoencoders* in *International conference on artificial neural networks* (2018), 412–422.
303. Kwon, Y., Yoo, J., Choi, Y.-S., Son, W.-J., Lee, D. & Kang, S. Efficient learning of non-autoregressive graph variational autoencoders for molecular graph generation. *Journal of Cheminformatics* **11**, 1–10 (2019).
304. Ma, T., Chen, J. & Xiao, C. Constrained generation of semantically valid graphs via regularizing variational autoencoders. *Advances in Neural Information Processing Systems* **31** (2018).
305. Bresson, X. & Laurent, T. A two-step graph convolutional decoder for molecule generation. *arXiv preprint arXiv:1906.03412* (2019).
306. Jin, W., Barzilay, R. & Jaakkola, T. *Junction tree variational autoencoder for molecular graph generation* in *International conference on machine learning* (2018), 2323–2332.
307. Jin, W., Barzilay, R. & Jaakkola, T. *Hierarchical generation of molecular graphs using structural motifs* in *International conference on machine learning* (2020), 4839–4848.

308. Li, Y., Hu, J., Wang, Y., Zhou, J., Zhang, L. & Liu, Z. Deepsccaffold: a comprehensive tool for scaffold-based de novo drug discovery using deep learning. *Journal of chemical information and modeling* **60**, 77–91 (2019).
309. Mahmood, O., Mansimov, E., Bonneau, R. & Cho, K. Masked graph modeling for molecule generation. *Nature communications* **12**, 1–12 (2021).
310. Kang, S. & Cho, K. Conditional molecular design with deep generative models. *Journal of chemical information and modeling* **59**, 43–52 (2018).
311. Lim, J., Ryu, S., Kim, J. W. & Kim, W. Y. Molecular generative model based on conditional variational autoencoder for de novo molecular design. *Journal of cheminformatics* **10**, 1–9 (2018).
312. Lee, M. & Min, K. MGCVAE: Multi-Objective Inverse Design via Molecular Graph Conditional Variational Autoencoder. *Journal of Chemical Information and Modeling* (2022).
313. Richards, R. & Groener, A. Conditional  $\beta$ -VAE for De Novo Molecular Generation (2022).
314. Griffiths, R.-R. & Hernández-Lobato, J. M. Constrained Bayesian optimization for automatic chemical design using variational autoencoders. *Chemical science* **11**, 577–586 (2020).
315. Samanta, B., De, A., Jana, G., Gómez, V., Chattaraj, P. K., Ganguly, N. & Gomez-Rodriguez, M. Nevae: A deep generative model for molecular graphs. *Journal of machine learning research. 2020 Apr; 21 (114): 1-33* (2020).
316. Hoffman, S. C., Chenthamarakshan, V., Wadhawan, K., Chen, P.-Y. & Das, P. Optimizing molecules using efficient queries from property evaluations. *Nature Machine Intelligence* **4**, 21–31 (2022).
317. Chenthamarakshan, V., Das, P., Hoffman, S., Strobel, H., Padhi, I., Lim, K. W., Hoover, B., Manica, M., Born, J., Laino, T., *et al.* CogMol: target-specific and selective drug design for COVID-19 using deep generative models. *Advances in Neural Information Processing Systems* **33**, 4320–4332 (2020).
318. Ragoza, M., Masuda, T. & Koes, D. R. Generating 3D molecules conditional on receptor binding sites with deep generative models. *Chemical science* **13**, 2701–2713 (2022).
319. Jin, W., Yang, K., Barzilay, R. & Jaakkola, T. *Learning Multimodal Graph-to-Graph Translation for Molecule Optimization* in *International Conference on Learning Representations* (2019).
320. Wang, H., Wang, J., Wang, J., Zhao, M., Zhang, W., Zhang, F., Li, W., Xie, X. & Guo, M. Learning graph representation with generative adversarial nets. *IEEE Transactions on Knowledge and Data Engineering* **33**, 3090–3103 (2019).
321. Guo, X., Wu, L. & Zhao, L. Deep graph translation. *IEEE Transactions on Neural Networks and Learning Systems* (2022).
322. Mirza, M. & Osindero, S. Conditional generative adversarial nets. *arXiv preprint arXiv:1411.1784* (2014).

323. Arjovsky, M., Chintala, S. & Bottou, L. *Wasserstein generative adversarial networks* in *International conference on machine learning* (2017), 214–223.
324. Karras, T., Laine, S. & Aila, T. *A style-based generator architecture for generative adversarial networks* in *Proceedings of the IEEE/CVF conference on computer vision and pattern recognition* (2019), 4401–4410.
325. De Cao, N. & Kipf, T. MolGAN: An implicit generative model for small molecular graphs. *arXiv preprint arXiv:1805.11973* (2018).
326. Maziarka, Ł., Pocha, A., Kaczmarszky, J., Rataj, K., Danel, T. & Warchoł, M. Mol-CycleGAN: a generative model for molecular optimization. *Journal of Cheminformatics* **12**, 1–18 (2020).
327. Zhu, J.-Y., Park, T., Isola, P. & Efros, A. A. *Unpaired image-to-image translation using cycle-consistent adversarial networks* in *Proceedings of the IEEE international conference on computer vision* (2017), 2223–2232.
328. Tsujimoto, Y., Hiwa, S., Nakamura, Y., Oe, Y. & Hiroyasu, T. L-MolGAN: An improved implicit generative model for large molecular graphs (2021).
329. Liu, J., Kumar, A., Ba, J., Kiros, J. & Swersky, K. Graph normalizing flows. *Advances in Neural Information Processing Systems* **32** (2019).
330. Kobyzhev, I., Prince, S. J. & Brubaker, M. A. Normalizing flows: An introduction and review of current methods. *IEEE transactions on pattern analysis and machine intelligence* **43**, 3964–3979 (2020).
331. Dinh, L., Krueger, D. & Bengio, Y. Nice: Non-linear independent components estimation. *arXiv preprint arXiv:1410.8516* (2014).
332. Dinh, L., Sohl-Dickstein, J. & Bengio, S. Density estimation using real nvp. *arXiv preprint arXiv:1605.08803* (2016).
333. Madhawa, K., Ishiguro, K., Nakago, K. & Abe, M. Graphnvp: An invertible flow model for generating molecular graphs. *arXiv preprint arXiv:1905.11600* (2019).
334. Zang, C. & Wang, F. MoFlow: an invertible flow model for generating molecular graphs in *Proceedings of the 26th ACM SIGKDD International Conference on Knowledge Discovery & Data Mining* (2020), 617–626.
335. Song, Y. & Ermon, S. Improved techniques for training score-based generative models. *Advances in neural information processing systems* **33**, 12438–12448 (2020).
336. Song, J., Meng, C. & Ermon, S. Denoising diffusion implicit models. *arXiv preprint arXiv:2010.02502* (2020).
337. Niu, C., Song, Y., Song, J., Zhao, S., Grover, A. & Ermon, S. Permutation invariant graph generation via score-based generative modeling in *International Conference on Artificial Intelligence and Statistics* (2020), 4474–4484.
338. Song, Y., Sohl-Dickstein, J., Kingma, D. P., Kumar, A., Ermon, S. & Poole, B. Score-based generative modeling through stochastic differential equations. *arXiv preprint arXiv:2011.13456* (2020).
339. Trippe, B. L., Yim, J., Tischer, D., Broderick, T., Baker, D., Barzilay, R. & Jaakkola, T. Diffusion probabilistic modeling of protein backbones

in 3D for the motif-scaffolding problem. *arXiv preprint arXiv:2206.04119* (2022).

- 340. Axelrod, S. & Gomez-Bombarelli, R. Molecular machine learning with conformer ensembles. *arXiv preprint arXiv:2012.08452* (2020).
- 341. Xu, Z., Luo, Y., Zhang, X., Xu, X., Xie, Y., Liu, M., Dickerson, K., Deng, C., Nakata, M. & Ji, S. Molecule3D: A Benchmark for Predicting 3D Geometries from Molecular Graphs. *arXiv preprint arXiv:2110.01717* (2021).
- 342. AlQuraishi, M. & Sorger, P. K. Differentiable biology: using deep learning for biophysics-based and data-driven modeling of molecular mechanisms. *Nature methods* **18**, 1169–1180 (2021).
- 343. Hawkins, P. C. Conformation generation: the state of the art. *Journal of chemical information and modeling* **57**, 1747–1756 (2017).
- 344. Shi, C., Luo, S., Xu, M. & Tang, J. *Learning gradient fields for molecular conformation generation* in *International Conference on Machine Learning* (2021), 9558–9568.
- 345. Xu, M., Yu, L., Song, Y., Shi, C., Ermon, S. & Tang, J. *GeoDiff: A Geometric Diffusion Model for Molecular Conformation Generation* in *International Conference on Learning Representations* (2022).
- 346. Kabsch, W. A solution for the best rotation to relate two sets of vectors. *Acta Crystallographica Section A: Crystal Physics, Diffraction, Theoretical and General Crystallography* **32**, 922–923 (1976).
- 347. Ganea, O., Pattanaik, L., Coley, C., Barzilay, R., Jensen, K., Green, W. & Jaakkola, T. Geomol: Torsional geometric generation of molecular 3d conformer ensembles. *Advances in Neural Information Processing Systems* **34**, 13757–13769 (2021).
- 348. Mansimov, E., Mahmood, O., Kang, S. & Cho, K. Molecular geometry prediction using a deep generative graph neural network. *Scientific reports* **9**, 1–13 (2019).
- 349. Simm, G. N. & Hernández-Lobato, J. M. A generative model for molecular distance geometry. *arXiv preprint arXiv:1909.11459* (2019).
- 350. Xu, M., Luo, S., Bengio, Y., Peng, J. & Tang, J. Learning neural generative dynamics for molecular conformation generation. *arXiv preprint arXiv:2102.10240* (2021).
- 351. Liberti, L., Lavor, C., Maculan, N. & Mucherino, A. Euclidean distance geometry and applications. *SIAM review* **56**, 3–69 (2014).
- 352. Xu, M., Wang, W., Luo, S., Shi, C., Bengio, Y., Gomez-Bombarelli, R. & Tang, J. *An end-to-end framework for molecular conformation generation via bilevel programming* in *International Conference on Machine Learning* (2021), 11537–11547.
- 353. Luo, S., Shi, C., Xu, M. & Tang, J. Predicting molecular conformation via dynamic graph score matching. *Advances in Neural Information Processing Systems* **34**, 19784–19795 (2021).
- 354. Jing, B., Corso, G., Chang, J., Barzilay, R. & Jaakkola, T. Torsional Diffusion for Molecular Conformer Generation. *arXiv preprint arXiv:2206.01729* (2022).

355. Gogineni, T., Xu, Z., Punzalan, E., Jiang, R., Kammeraad, J., Tewari, A. & Zimmerman, P. Torsionnet: A reinforcement learning approach to sequential conformer search. *Advances in Neural Information Processing Systems* **33**, 20142–20153 (2020).
356. Kadurin, A., Nikolenko, S., Khrabrov, K., Aliper, A. & Zhavoronkov, A. druGAN: an advanced generative adversarial autoencoder model for de novo generation of new molecules with desired molecular properties in silico. *Molecular pharmaceutics* **14**, 3098–3104 (2017).
357. Segler, M. H., Kogej, T., Tyrchan, C. & Waller, M. P. Generating focused molecule libraries for drug discovery with recurrent neural networks. *ACS central science* **4**, 120–131 (2018).
358. Prykhodko, O., Johansson, S. V., Kotsias, P.-C., Arús-Pous, J., Bjerrum, E. J., Engkvist, O. & Chen, H. A de novo molecular generation method using latent vector based generative adversarial network. *Journal of Cheminformatics* **11**, 1–13 (2019).
359. Coley, C. W., Barzilay, R., Jaakkola, T. S., Green, W. H. & Jensen, K. F. Prediction of organic reaction outcomes using machine learning. *ACS central science* **3**, 434–443 (2017).
360. Corey, E. J. General methods for the construction of complex molecules. *Pure and Applied chemistry* **14**, 19–38 (1967).
361. Coley, C. W., Green, W. H. & Jensen, K. F. Machine learning in computer-aided synthesis planning. *Accounts of chemical research* **51**, 1281–1289 (2018).
362. Schneider, N., Stiefl, N. & Landrum, G. A. What's what: The (nearly) definitive guide to reaction role assignment. *Journal of chemical information and modeling* **56**, 2336–2346 (2016).
363. Shi, C., Xu, M., Guo, H., Zhang, M. & Tang, J. *A graph to graphs framework for retrosynthesis prediction* in *International conference on machine learning* (2020), 8818–8827.
364. Sun, R., Dai, H., Li, L., Kearnes, S. & Dai, B. Energy-based view of retrosynthesis. *arXiv preprint arXiv:2007.13437* (2020).
365. Somnath, V. R., Bunne, C., Coley, C., Krause, A. & Barzilay, R. Learning graph models for retrosynthesis prediction. *Advances in Neural Information Processing Systems* **34**, 9405–9415 (2021).
366. Lin, Z., Yin, S., Shi, L., Zhou, W. & Zhang, Y. G2GT: Retrosynthesis Prediction with Graph to Graph Attention Neural Network and Self-Training. *arXiv preprint arXiv:2204.08608* (2022).
367. Han, P., Zhao, P., Lu, C., Huang, J., Wu, J., Shang, S., Yao, B. & Zhang, X. *GNN-Retro: Retrosynthetic Planning with Graph Neural Networks* in *Proceedings of the AAAI Conference on Artificial Intelligence* **36** (2022), 4014–4021.
368. Do, K., Tran, T. & Venkatesh, S. *Graph transformation policy network for chemical reaction prediction* in *Proceedings of the 25th ACM SIGKDD International Conference on Knowledge Discovery & Data Mining* (2019), 750–760.

369. Sacha, M., Błaz, M., Byrski, P., Dabrowski-Tumanski, P., Chrominski, M., Loska, R., Włodarczyk-Pruszynski, P. & Jastrzebski, S. Molecule edit graph attention network: modeling chemical reactions as sequences of graph edits. *Journal of Chemical Information and Modeling* **61**, 3273–3284 (2021).
370. Ryou, S., Maser, M. R., Cui, A. Y., DeLano, T. J., Yue, Y. & Reisman, S. E. Graph Neural Networks for the Prediction of Substrate-Specific Organic Reaction Conditions. *arXiv preprint arXiv:2007.04275* (2020).
371. Saebi, M., Nan, B., Herr, J., Wahlers, J., Wiest, O. & Chawla, N. Graph neural networks for predicting chemical reaction performance (2021).
372. Kwon, Y., Lee, D., Choi, Y.-S. & Kang, S. Uncertainty-aware prediction of chemical reaction yields with graph neural networks. *Journal of Cheminformatics* **14**, 1–10 (2022).
373. Bradshaw, J., Paige, B., Kusner, M. J., Segler, M. & Hernández-Lobato, J. M. A model to search for synthesizable molecules. *Advances in Neural Information Processing Systems* **32** (2019).
374. Gu, G. H., Jang, J., Noh, J., Walsh, A. & Jung, Y. Perovskite synthesizability using graph neural networks. *npj Computational Materials* **8**, 1–8 (2022).
375. Liu, C.-H., Korablyov, M., Jastrzębski, S., Włodarczyk-Pruszyński, P., Bengio, Y. & Segler, M. RetroGNN: Fast Estimation of Synthesizability for Virtual Screening and De Novo Design by Learning from Slow Retrosynthesis Software. *Journal of Chemical Information and Modeling* **62**, 2293–2300 (2022).
376. Miller, G. A. WordNet: a lexical database for English. *Communications of the ACM* **38**, 39–41 (1995).
377. Lehmann, J., Isele, R., Jakob, M., Jentzsch, A., Kontokostas, D., Mendes, P. N., Hellmann, S., Morsey, M., Van Kleef, P., Auer, S., *et al.* Dbpedia—a large-scale, multilingual knowledge base extracted from wikipedia. *Semantic web* **6**, 167–195 (2015).
378. Ryu, J. Y., Kim, H. U. & Lee, S. Y. Deep learning improves prediction of drug-drug and drug-food interactions. *Proceedings of the National Academy of Sciences* **115**, E4304–E4311 (2018).
379. Niu, J., Straubinger, R. M. & Mager, D. E. Pharmacodynamic drug–drug interactions. *Clinical Pharmacology & Therapeutics* **105**, 1395–1406 (2019).
380. Karim, M. R., Cochez, M., Jares, J. B., Uddin, M., Beyan, O. & Decker, S. *Drug-drug interaction prediction based on knowledge graph embeddings and convolutional-LSTM network* in *Proceedings of the 10th ACM international conference on bioinformatics, computational biology and health informatics* (2019), 113–123.
381. Celebi, R., Uyar, H., Yasar, E., Gumus, O., Dikenelli, O. & Dumontier, M. Evaluation of knowledge graph embedding approaches for drug-drug interaction prediction in realistic settings. *BMC bioinformatics* **20**, 1–14 (2019).

382. Zhang, Z., Chen, L., Zhong, F., Wang, D., Jiang, J., Zhang, S., Jiang, H., Zheng, M. & Li, X. Graph neural network approaches for drug-target interactions. *Current Opinion in Structural Biology* **73**, 102327 (2022).

383. Wishart, D. S., Feunang, Y. D., Guo, A. C., Lo, E. J., Marcu, A., Grant, J. R., Sajed, T., Johnson, D., Li, C., Sayeeda, Z., *et al.* DrugBank 5.0: a major update to the DrugBank database for 2018. *Nucleic acids research* **46**, D1074–D1082 (2018).

384. Kanehisa, M. & Goto, S. KEGG: kyoto encyclopedia of genes and genomes. *Nucleic acids research* **28**, 27–30 (2000).

385. Kanehisa, M., Furumichi, M., Sato, Y., Ishiguro-Watanabe, M. & Tanabe, M. KEGG: integrating viruses and cellular organisms. *Nucleic acids research* **49**, D545–D551 (2021).

386. Zitnik, M., Sosič, R., Maheshwari, S. & Leskovec, J. *BioSNAP Datasets: Stanford Biomedical Network Dataset Collection 2018*. <http://snap.stanford.edu/biodata>.

387. Whirl-Carrillo, M., McDonagh, E. M., Hebert, J., Gong, L., Sangkuhl, K., Thorn, C., Altman, R. B. & Klein, T. E. Pharmacogenomics knowledge for personalized medicine. *Clinical Pharmacology & Therapeutics* **92**, 414–417 (2012).

388. Whirl-Carrillo, M., Huddart, R., Gong, L., Sangkuhl, K., Thorn, C. F., Whaley, R. & Klein, T. E. An evidence-based framework for evaluating pharmacogenomics knowledge for personalized medicine. *Clinical Pharmacology & Therapeutics* **110**, 563–572 (2021).

389. Belleau, F., Nolin, M.-A., Tourigny, N., Rigault, P. & Morissette, J. Bio2RDF: towards a mashup to build bioinformatics knowledge systems. *Journal of biomedical informatics* **41**, 706–716 (2008).

390. Feng, Y.-H., Zhang, S.-W. & Shi, J.-Y. DPDDI: a deep predictor for drug-drug interactions. *BMC bioinformatics* **21**, 1–15 (2020).

391. Yu, Y., Huang, K., Zhang, C., Glass, L. M., Sun, J. & Xiao, C. SumGNN: multi-typed drug interaction prediction via efficient knowledge graph summarization. *Bioinformatics* **37**, 2988–2995 (2021).

392. Bai, Y., Gu, K., Sun, Y. & Wang, W. Bi-level graph neural networks for drug-drug interaction prediction. *arXiv preprint arXiv:2006.14002* (2020).

393. Chen, Y., Ma, T., Yang, X., Wang, J., Song, B. & Zeng, X. MUFFIN: multi-scale feature fusion for drug–drug interaction prediction. *Bioinformatics* **37**, 2651–2658 (2021).

394. Lyu, T., Gao, J., Tian, L., Li, Z., Zhang, P. & Zhang, J. *MDNN: A Multi-modal Deep Neural Network for Predicting Drug-Drug Interaction Events*. in *IJCAI* (2021), 3536–3542.

395. Lin, X., Quan, Z., Wang, Z.-J., Ma, T. & Zeng, X. *KGNN: Knowledge Graph Neural Network for Drug-Drug Interaction Prediction*. in *IJCAI* **380** (2020), 2739–2745.

396. Zhang, Y., Li, Z., Duan, B., Qin, L. & Peng, J. MKGE: Knowledge Graph Embedding with Molecular Structure Information. *Computational Biology and Chemistry*, 107730 (2022).

397. He, C., Liu, Y., Li, H., Zhang, H., Mao, Y., Qin, X., Liu, L. & Zhang, X. Multi-type feature fusion based on graph neural network for drug-drug interaction prediction. *BMC Bioinformatics* **23**, 1–18 (2022).
398. Feng, Y.-H. & Zhang, S.-W. Prediction of Drug-Drug Interaction Using an Attention-Based Graph Neural Network on Drug Molecular Graphs. *Molecules* **27**, 3004 (2022).
399. Nyamabo, A. K., Yu, H. & Shi, J.-Y. SSI-DDI: substructure–substructure interactions for drug–drug interaction prediction. *Briefings in Bioinformatics* **22**, bbab133 (2021).
400. Nyamabo, A. K., Yu, H., Liu, Z. & Shi, J.-Y. Drug–drug interaction prediction with learnable size-adaptive molecular substructures. *Briefings in Bioinformatics* **23**, bbab441 (2022).
401. Keskin, O., Nussinov, R. & Gursoy, A. in *Functional Proteomics* 505–521 (Springer, 2008).
402. Zitnik, M., Sosič, R., Feldman, M. W. & Leskovec, J. Evolution of resilience in protein interactomes across the tree of life. *Proceedings of the National Academy of Sciences* **116**, 4426–4433 (2019).
403. Yang, F., Fan, K., Song, D. & Lin, H. Graph-based prediction of Protein-protein interactions with attributed signed graph embedding. *BMC bioinformatics* **21**, 1–16 (2020).
404. Garay-Ruiz, D. & Bo, C. Chemical reaction network knowledge graphs: the OntoRXN ontology. *Journal of Cheminformatics* **14**, 1–12 (2022).
405. Zitnik, M., Agrawal, M. & Leskovec, J. Modeling polypharmacy side effects with graph convolutional networks. *Bioinformatics* **34**, i457–i466 (2018).
406. Jumper, J., Evans, R., Pritzel, A., Green, T., Figurnov, M., Ronneberger, O., Tunyasuvunakool, K., Bates, R., Žídek, A., Potapenko, A., *et al.* Highly accurate protein structure prediction with AlphaFold. *Nature* **596**, 583–589 (2021).
407. Baek, M., DiMaio, F., Anishchenko, I., Dauparas, J., Ovchinnikov, S., Lee, G. R., Wang, J., Cong, Q., Kinch, L. N., Schaeffer, R. D., *et al.* Accurate prediction of protein structures and interactions using a three-track neural network. *Science* **373**, 871–876 (2021).
408. Mirdita, M., Schütze, K., Moriwaki, Y., Heo, L., Ovchinnikov, S. & Steineger, M. ColabFold: making protein folding accessible to all. *Nature Methods*, 1–4 (2022).
409. Lin, Z., Akin, H., Rao, R., Hie, B., Zhu, Z., Lu, W., dos Santos Costa, A., Fazel-Zarandi, M., Sercu, T., Candido, S., *et al.* Language models of protein sequences at the scale of evolution enable accurate structure prediction. *bioRxiv* (2022).
410. Wu, R., Ding, F., Wang, R., Shen, R., Zhang, X., Luo, S., Su, C., Wu, Z., Xie, Q., Berger, B., *et al.* High-resolution de novo structure prediction from primary sequence. *bioRxiv* (2022).

411. Spalević, S., Veličković, P., Kovačević, J. & Nikolić, M. Hierarchical protein function prediction with tail-GNNs. *arXiv preprint arXiv:2007.12804* (2020).
412. Gligorijević, V., Renfrew, P. D., Kosciolek, T., Leman, J. K., Berenberg, D., Vatanen, T., Chandler, C., Taylor, B. C., Fisk, I. M., Vlamakis, H., *et al.* Structure-based protein function prediction using graph convolutional networks. *Nature communications* **12**, 1–14 (2021).
413. Zhang, Z., Xu, M., Jamasb, A., Chenthamarakshan, V., Lozano, A., Das, P. & Tang, J. Protein representation learning by geometric structure pre-training. *arXiv preprint arXiv:2203.06125* (2022).
414. Evans, R., O'Neill, M., Pritzel, A., Antropova, N., Senior, A. W., Green, T., Žídek, A., Bates, R., Blackwell, S., Yim, J., *et al.* Protein complex prediction with AlphaFold-Multimer. *BioRxiv* (2021).
415. Wang, X., Flannery, S. T. & Kihara, D. Protein docking model evaluation by graph neural networks. *Frontiers in Molecular Biosciences*, 402 (2021).
416. Yan, Z., Hamilton, W. L. & Blanchette, M. Graph neural representational learning of RNA secondary structures for predicting RNA-protein interactions. *Bioinformatics* **36**, i276–i284 (2020).
417. Bryant, P., Pozzati, G. & Eloffson, A. Improved prediction of protein-protein interactions using AlphaFold2. *Nature communications* **13**, 1–11 (2022).
418. Jing, B., Eismann, S., Suriana, P., Townshend, R. J. & Dror, R. Learning from protein structure with geometric vector perceptrons. *arXiv preprint arXiv:2009.01411* (2020).
419. Ingraham, J., Garg, V., Barzilay, R. & Jaakkola, T. Generative models for graph-based protein design. *Advances in neural information processing systems* **32** (2019).
420. Strokach, A., Becerra, D., Corbi-Verge, C., Perez-Riba, A. & Kim, P. M. Fast and flexible protein design using deep graph neural networks. *Cell systems* **11**, 402–411 (2020).
421. Anand, N. & Achim, T. Protein Structure and Sequence Generation with Equivariant Denoising Diffusion Probabilistic Models. *arXiv preprint arXiv:2205.15019* (2022).
422. Townshend, R. J., Vögele, M., Suriana, P., Derry, A., Powers, A., Laloudakis, Y., Balachandar, S., Jing, B., Anderson, B., Eismann, S., *et al.* Atom3d: Tasks on molecules in three dimensions. *arXiv preprint arXiv:2012.04035* (2020).
423. Wang, J., Ma, A., Chang, Y., Gong, J., Jiang, Y., Qi, R., Wang, C., Fu, H., Ma, Q. & Xu, D. scGNN is a novel graph neural network framework for single-cell RNA-Seq analyses. *Nature communications* **12**, 1–11 (2021).
424. Townshend, R. J., Eismann, S., Watkins, A. M., Rangan, R., Karelina, M., Das, R. & Dror, R. O. Geometric deep learning of RNA structure. *Science* **373**, 1047–1051 (2021).

425. Reymond, J.-L., Ruddigkeit, L., Blum, L. & Van Deursen, R. The enumeration of chemical space. *Wiley Interdisciplinary Reviews: Computational Molecular Science* **2**, 717–733 (2012).
426. Hadsell, R., Chopra, S. & LeCun, Y. Dimensionality reduction by learning an invariant mapping in *Proceedings of the IEEE/CVF Conference on Computer Vision and Pattern Recognition* **2** (2006), 1735–1742.
427. Doersch, C. & Zisserman, A. Multi-task self-supervised visual learning in *Proceedings of the IEEE International Conference on Computer Vision* (2017), 2051–2060.
428. Zhang, R., Isola, P. & Efros, A. A. Colorful image colorization in *European conference on computer vision* (2016), 649–666.
429. Gidaris, S., Singh, P. & Komodakis, N. Unsupervised representation learning by predicting image rotations. *arXiv preprint arXiv:1803.07728* (2018).
430. Pathak, D., Krahenbuhl, P., Donahue, J., Darrell, T. & Efros, A. A. Context encoders: Feature learning by inpainting in *Proceedings of the IEEE conference on computer vision and pattern recognition* (2016), 2536–2544.
431. Zhang, R., Isola, P. & Efros, A. A. Split-brain autoencoders: Unsupervised learning by cross-channel prediction in *Proceedings of the IEEE conference on computer vision and pattern recognition* (2017), 1058–1067.
432. Bao, H., Dong, L., Piao, S. & Wei, F. BEiT: BERT Pre-Training of Image Transformers in *International Conference on Learning Representations* (2022).
433. He, K., Chen, X., Xie, S., Li, Y., Dollár, P. & Girshick, R. Masked autoencoders are scalable vision learners in *Proceedings of the IEEE/CVF Conference on Computer Vision and Pattern Recognition* (2022), 16000–16009.
434. Devlin, J., Chang, M.-W., Lee, K. & Toutanova, K. Bert: Pre-training of deep bidirectional transformers for language understanding. *arXiv preprint arXiv:1810.04805* (2018).
435. Liu, Y., Ott, M., Goyal, N., Du, J., Joshi, M., Chen, D., Levy, O., Lewis, M., Zettlemoyer, L. & Stoyanov, V. Roberta: A robustly optimized bert pretraining approach. *arXiv preprint arXiv:1907.11692* (2019).
436. He, K., Fan, H., Wu, Y., Xie, S. & Girshick, R. Momentum contrast for unsupervised visual representation learning in *Proceedings of the IEEE/CVF conference on computer vision and pattern recognition* (2020), 9729–9738.
437. Chen, T., Kornblith, S., Norouzi, M. & Hinton, G. A simple framework for contrastive learning of visual representations in *International conference on machine learning* (2020), 1597–1607.
438. Caron, M., Misra, I., Mairal, J., Goyal, P., Bojanowski, P. & Joulin, A. Unsupervised learning of visual features by contrasting cluster assignments. *Advances in Neural Information Processing Systems* **33**, 9912–9924 (2020).
439. Bengio, Y., Lecun, Y. & Hinton, G. Deep learning for AI. *Communications of the ACM* **64**, 58–65 (2021).

440. Xie, S., Gu, J., Guo, D., Qi, C. R., Guibas, L. & Litany, O. *Pointcontrast: Unsupervised pre-training for 3d point cloud understanding* in *European conference on computer vision* (2020), 574–591.
441. Chaitanya, K., Erdil, E., Karani, N. & Konukoglu, E. Contrastive learning of global and local features for medical image segmentation with limited annotations. *Advances in Neural Information Processing Systems* **33**, 12546–12558 (2020).
442. Gao, T., Yao, X. & Chen, D. Simcse: Simple contrastive learning of sentence embeddings. *arXiv preprint arXiv:2104.08821* (2021).
443. You, Y., Chen, T., Sui, Y., Chen, T., Wang, Z. & Shen, Y. Graph contrastive learning with augmentations. *Advances in Neural Information Processing Systems* **33**, 5812–5823 (2020).
444. Magar, R., Wang, Y. & Farimani, A. B. Crystal Twins: Self-supervised Learning for Crystalline Material Property Prediction. *arXiv preprint arXiv:2205.01893* (2022).
445. Grill, J.-B., Strub, F., Altché, F., Tallec, C., Richemond, P., Buchatskaya, E., Doersch, C., Avila Pires, B., Guo, Z., Gheshlaghi Azar, M., *et al.* Bootstrap your own latent-a new approach to self-supervised learning. *Advances in neural information processing systems* **33**, 21271–21284 (2020).
446. Chen, X. & He, K. *Exploring simple siamese representation learning* in *Proceedings of the IEEE/CVF Conference on Computer Vision and Pattern Recognition* (2021), 15750–15758.
447. Zbontar, J., Jing, L., Misra, I., LeCun, Y. & Deny, S. *Barlow twins: Self-supervised learning via redundancy reduction* in *International Conference on Machine Learning* (2021), 12310–12320.
448. Bardes, A., Ponce, J. & LeCun, Y. Vicreg: Variance-invariance-covariance regularization for self-supervised learning. *arXiv preprint arXiv:2105.04906* (2021).
449. Xie, Y., Xu, Z., Zhang, J., Wang, Z. & Ji, S. Self-supervised learning of graph neural networks: A unified review. *IEEE Transactions on Pattern Analysis and Machine Intelligence* (2022).
450. Fang, Y., Zhang, Q., Chen, Z., Fan, X. & Chen, H. Knowledge-informed Molecular Learning: A Survey on Paradigm Transfer. *arXiv preprint arXiv:2202.10587* (2022).
451. Zhang, Z., Liu, Q., Wang, H., Lu, C. & Lee, C.-K. *Motif-based Graph Self-Supervised Learning for Molecular Property Prediction* in *Advances in Neural Information Processing Systems* **34** (2021).
452. He, J., Tian, K., Luo, S., Min, Y., Zheng, S., Shi, Y., He, D., Liu, H., Yu, N., Wang, L., *et al.* Masked Molecule Modeling: A New Paradigm of Molecular Representation Learning for Chemistry Understanding (2022).
453. Liu, S., Demirel, M. F. & Liang, Y. N-gram graph: Simple unsupervised representation for graphs, with applications to molecules. *Advances in neural information processing systems* **32** (2019).
454. Sun, F.-Y., Hoffman, J., Verma, V. & Tang, J. *InfoGraph: Unsupervised and Semi-supervised Graph-Level Representation Learning via Mutual In-*

*formation Maximization in International Conference on Learning Representations* (2019).

- 455. Li, S., Zhou, J., Xu, T., Dou, D. & Xiong, H. *GeomGCL: Geometric Graph Contrastive Learning for Molecular Property Prediction* in *Proceedings of the AAAI Conference on Artificial Intelligence* **36** (2022), 4541–4549.
- 456. Zhou, G., Gao, Z., Ding, Q., Zheng, H., Xu, H., Wei, Z., Zhang, L. & Ke, G. Uni-Mol: A Universal 3D Molecular Representation Learning Framework (2022).
- 457. Liu, S., Wang, H., Liu, W., Lasenby, J., Guo, H. & Tang, J. *Pre-training Molecular Graph Representation with 3D Geometry* in *International Conference on Learning Representations* (2022).
- 458. Stärk, H., Beaini, D., Corso, G., Tossou, P., Dallago, C., Günnemann, S. & Lió, P. *3D Infomax improves GNNs for Molecular Property Prediction* in *Proceedings of the 39th International Conference on Machine Learning* (2022).
- 459. Zaidi, S., Schaarschmidt, M., Martens, J., Kim, H., Teh, Y. W., Sanchez-Gonzalez, A., Battaglia, P., Pascanu, R. & Godwin, J. Pre-training via Denoising for Molecular Property Prediction. *arXiv preprint arXiv:2206.00133* (2022).
- 460. Liu, S., Guo, H. & Tang, J. Molecular Geometry Pretraining with SE(3)-Invariant Denoising Distance Matching. *arXiv preprint arXiv:2206.13602* (2022).
- 461. Jiao, R., Han, J., Huang, W., Rong, Y. & Liu, Y. 3D Equivariant Molecular Graph Pretraining. *arXiv preprint arXiv:2207.08824* (2022).
- 462. Chen, D., Gao, K., Nguyen, D. D., Chen, X., Jiang, Y., Wei, G.-W. & Pan, F. Algebraic graph-assisted bidirectional transformers for molecular property prediction. *Nature Communications* **12**, 1–9 (2021).
- 463. Zhang, S., Hu, Z., Subramonian, A. & Sun, Y. Motif-driven contrastive learning of graph representations. *arXiv preprint arXiv:2012.12533* (2020).
- 464. Zhu, J., Xia, Y., Qin, T., Zhou, W., Li, H. & Liu, T.-Y. Dual-view Molecule Pre-training. *arXiv preprint arXiv:2106.10234* (2021).
- 465. Zhu, Y., Chen, D., Du, Y., Wang, Y., Liu, Q. & Wu, S. *Featurizations Matter: A Multiview Contrastive Learning Approach to Molecular Pretraining* in *ICML 2022 2nd AI for Science Workshop* (2022).
- 466. Wang, Y., Magar, R., Liang, C. & Barati Farimani, A. Improving Molecular Contrastive Learning via Faulty Negative Mitigation and Decomposed Fragment Contrast. *Journal of Chemical Information and Modeling* (2022).
- 467. Fang, Y., Yang, H., Zhuang, X., Shao, X., Fan, X. & Chen, H. Knowledge-aware contrastive molecular graph learning. *arXiv preprint arXiv:2103.13047* (2021).
- 468. Sun, M., Xing, J., Wang, H., Chen, B. & Zhou, J. *MoCL: data-driven molecular fingerprint via knowledge-aware contrastive learning from molecular graph* in *Proceedings of the 27th ACM SIGKDD Conference on Knowledge Discovery & Data Mining* (2021), 3585–3594.

469. Fang, Y., Zhang, Q., Yang, H., Zhuang, X., Deng, S., Zhang, W., Qin, M., Chen, Z., Fan, X. & Chen, H. *Molecular contrastive learning with chemical element knowledge graph* in *Proceedings of the AAAI Conference on Artificial Intelligence* **36** (2022), 3968–3976.
470. Gao, Z., Tan, C., Wu, L. & Li, S. Z. CoSP: Co-supervised pretraining of pocket and ligand. *arXiv preprint arXiv:2206.12241* (2022).